

1
2
3
4
5
6
7
8
9
10
11
12
13
14
15
16
17
18
19
20
21
22
23
24
25
26
27
28

PROFESSOR J. SIMMER (Orcid ID : 0000-0002-7192-6105)

Article type : Original Paper

October 11, 2018

Corresponding author mail id :- jsimmer@umich.edu

Drs. Julia Clarke, Thomas Gillingwater, Anthony Graham, and Stefan Milz
Editors, *Journal of Anatomy*

Dear Editors,

The authors thank you and the reviewers for their very kind and generous comments about the paper (Quantitative Analysis of the Core 2D Arrangement and Distribution of Enamel Rods in Cross Sections of Mandibular Mouse Incisors), and for the very prompt review. We have addressed points raised by the two reviewers and describe the revisions below. All revisions are highlighted in yellow in the text of the revised manuscript.

1) Please consider combining some of your figures to reduce the overall figure count (15 would be regarded as excessive for a paper of this length)

Response: We have reduced the 15 figures to 10 figures and a table, and adjusted the text and legends accordingly.

This is the author manuscript accepted for publication and has undergone full peer review but has not been through the copyediting, typesetting, pagination and proofreading process, which may lead to differences between this version and the [Version of Record](#). Please cite this article as [doi: 10.1111/joa.12912](https://doi.org/10.1111/joa.12912)

This article is protected by copyright. All rights reserved

1
2
3
4
5
6
7
8
9
10
11
12
13
14
15
16
17
18
19
20
21
22
23
24
25
26
27
28
29
30
31

Referee: 1

2) The only concern relates to the authors second sentence in the abstract suggesting there is controversy in the literature as to whether individual ameloblasts create single enamel rods. More references discussing data supporting or questioning this theory/idea of a single cell responsible for single rod should be included, and the authors should, based on their data, make a clear statement of what they believe is the case.

Response: We apologize for the lack of clarity that caused this concern. We did not intend to cast doubt on the well-established conclusion that 1 ameloblast creates a single enamel rod. To the contrary, we intended to note that because each rod is produced by a single cell and represents the “fossilized path traced out by the Tomes' processes of the ameloblasts during enamel secretion” [Boyde A 1967. The development of enamel structure. *Proc R Soc Med*, **60**, 923-8], abundant information is thus preserved in the enamel structure concerning its formation.

The abstract is revised: “This has important implications concerning cell movement during the secretory stage because each ameloblast makes one enamel rod.”

The introduction is revised: “Each enamel rod traces the path followed by a single ameloblast (Boyde, 1967; Boyde, 1969; Smith and Warshawsky, 1977; Risnes et al., 2002; Skobe, 2006).”

Referee: 2

3) Well done. I found this to be a very well executed study and compellingly written manuscript. (no revisions requested).

All 10 figures are provided at TIFF files, 900 dpi.

Thanks again for your kind and prompt review of this manuscript.

Sincerely yours,



James P. Simmer, DDS, PhD

Biologic and Materials Sciences

University of Michigan School of Dentistry

1 Email: jsimmer@umich.edu

2
3 Quantitative Analysis of the Core 2D Arrangement and Distribution of Enamel
4 Rods in Cross Sections of Mandibular Mouse Incisors

5
6 Charles E. Smith^{1,2}, Yuanyuan Hu¹, Jan C-C. Hu¹ and James P. Simmer¹

7
8 ¹Department of Biologic and Materials Sciences, University of Michigan School of Dentistry, 1210
9 Eisenhower Place, Ann Arbor, Michigan USA 48108

10 ²Department of Anatomy & Cell Biology, Faculty of Medicine, McGill University, 3640 University Street,
11 Montreal, QC CANADA H3A 0C7

12
13 Charles E. Smith: charles.smith@mcgill.ca, +1-514-398 4520

14 Yuanyuan Hu: yyhu@umich.edu, +1-734-975 9326

15 Jan C-C Hu: janhu@umich.edu, +1-734-763 6769

16 James P. Simmer: jsimmer@umich.edu, +1-734-764 4676

17
18 Corresponding Author: James P. Simmer: jsimmer@umich.edu, +1-734-764-4676

19 Word Count: Abstract: 381 Main Text: 7018

20 Running Title: Core Arrangement of Enamel Rods in Mandibular Mouse Incisors

21
22
23 **Abstract**

24 Considerable descriptive information about the overall organization of mouse mandibular incisor
25 enamel is available but almost nothing is known about the quantitative characteristics of enamel rod

1 arrangement and distribution in these teeth. This has important implications concerning cell movement
2 during the secretory stage because each ameloblast makes one enamel rod. Knowing how many enamel
3 rods are cut open in a cross section of the enamel layer could provide insights into understanding the
4 dynamics of how groups of ameloblasts form the enamel layer. In this study, cross sections of fully
5 mineralized enamel were made on 24 mandibular mouse incisors, polished and etched, and imaged by
6 scanning electron microscopy in backscatter mode (BEI). Montaged maps of the entire enamel layer
7 were made at high magnification and the enamel rod profiles in each map were color coded based upon
8 rod category. Quantitative analyses of each color layer in the maps were then performed using standard
9 routines available in ImageJ. The data indicated that that there were on average $7,233 \pm 575$ enamel rod
10 profiles per cross section in mandibular incisors of 7-week-old mice with 70% located in the inner
11 enamel layer, 27% located in the outer enamel layer, and 3% positioned near the mesial and lateral
12 cementoenamel junctions. All enamel rod profiles showed progressive increases in tilt angles, some very
13 large in magnitude, from the lateral to mesial sides of the enamel layer whereas only minor variations in
14 tilt angle were found relative to enamel thickness at given locations across the enamel layer. The
15 decussation angle between alternating rows of rod profiles within the inner enamel layer was fairly
16 constant from the lateral to central labial sides of the enamel layer, but it increased dramatically in the
17 mesial region of the enamel layer. The packing density of all rod profiles decreased from lateral to
18 central labial regions of the enamel layer and then in progressing mesially either decreased slightly
19 (inner enamel, mesial tilt), increased slightly (outer enamel layer) or almost doubled in magnitude (inner
20 enamel, lateral tilt). It was concluded that these variations in rod tilt angle and packing densities are
21 adaptations that allow the tooth to maintain a sharp incisal edge and shovel-shape as renewing
22 segments formed by around 7,200 ameloblasts are brought onto the occluding surface of the tooth by
23 continuous renewal.

24 **Keywords:** Enamel formation, enamel rods, spatial distribution, quantification, rod decussation

26 Introduction

27 For over half a century the continuously erupting incisors of rats and mice have served as a very useful
28 model system for characterizing major cellular, structural, functional and chemical events that are
29 crucial to forming fully mineralized dentin and enamel layers (Schour and Massler, 1949; Smith and
30 Nanci, 1989; Smith, 1998; Jernvall and Thesleff, 2012; Kuang-Hsien Hu et al., 2014; Peterkova et al.,
31 2014; Pugach and Gibson, 2014; Renvoisé and Michon, 2014; Klein et al., 2017; Seidel et al., 2017). It is

1 evident from such literature that several developmental modifications evolved to tooth shape and
2 structural organization of hard tissues to accommodate the sideways as opposed to vertical eruptive
3 tooth movement more typical of most mammalian teeth (Jernvall and Thesleff, 2012; Kuang-Hsien Hu et
4 al., 2014; Peterkova et al., 2014; Renvoisé and Michon, 2014). Among the modifications made to enamel
5 development were changes in the way ameloblasts organize themselves spatially as they differentiate so
6 they eventually go on to form linear sheets of enamel rods stacked progressively one behind each other
7 all welded together by interrod enamel matrix (Warshawsky, 1971; Jodaikin et al., 1984; von
8 Koenigswald, 1985; Boyde, 1989; Martin, 1999; Cox, 2013; Nishikawa, 2017). Each sheet is angled in
9 alternating mesial and lateral directions (decussating) and in the case of current living mice and rats
10 tilted forward within the eruptive plane (angled toward incisal tip of tooth) (Warshawsky and Smith,
11 1971; von Koenigswald, 1985; Moinichen et al., 1996; Martin, 1999; Cox, 2013; Kuang-Hsien Hu et al.,
12 2014). This is opposed to the more common situation as seen for example in mouse molars where
13 groups of ameloblast form widely divergent enamel rod patterns at different sites across the crown
14 surface some of which show decussating arrangements (Boyde, 1989; Lyngstadaas et al., 1998; von
15 Koenigswald, 2004). This subtle bioengineering modification of forming incisally tilted sheets of enamel
16 rods having alternated side-to-side angulations (laminated) achieves two clear purposes, (1) it provides a
17 partial fracture plane along the outer enamel portions of the enamel rods that keeps the incisal tip
18 edges sharp for gnawing and (2) it provides considerable abrasion and especially fracture resistance
19 across the sheeted inner enamel portions and radially oriented outer enamel portions as the enamel
20 layer is worn away by attrition at the incisal edges (Warshawsky and Smith, 1971; von Koenigswald,
21 1985; Martin, 1999; Vieytes et al., 2007; Habelitz, 2015; Yilmaz et al., 2015).

22 Each enamel rod traces the path followed by a single ameloblast (Boyde, 1967; Boyde, 1969;
23 Smith and Warshawsky, 1977; Risnes et al., 2002; Skobe, 2006). As noted above, a great deal of
24 descriptive information currently exists about ameloblasts and how they form and help mineralize the
25 enamel layer and how the enamel rods they create form a variety of structural arrangements in 2D and
26 3D space. What has been missing from this literature is any kind of perspective about the quantities of
27 enamel rods cut open in a typical cross section from either mouse or rat incisors. Such information
28 would be very useful to advancing the understanding the cell population dynamics of amelogenesis, that
29 is, how groups of ameloblasts, rather than single ameloblasts, make the enamel layer (Smith and
30 Warshawsky, 1976; Smith and Warshawsky, 1977; Cox, 2013). The purpose of this project was to answer
31 one simple question about rat or mouse incisor amelogenesis: can all rod profiles exposed in a single
32 cross sectional (transverse) slice of mature rodent incisor enamel be identified and counted without

1 having a huge variation that would render the results unreliable. We opted to use the continuously
2 erupting mandibular incisors of mice to probe this question in part because the overall thickness of the
3 enamel layer in young adult mice (7-week-old) is similar to the thickness of the enamel layer present in
4 juvenile rats (100 g body weight) for which considerable quantitative data about cell renewal is available
5 (Smith and Warshawsky, 1975; Smith and Warshawsky, 1977) but the diameter and length of the
6 incisors in mice is about one-half the dimensions in rats making them less tedious to quantify
7 (Moinichen et al., 1996). As this report will document, the answer proved very surprising. Rod profiles in
8 cross sections of mandibular mouse incisor enamel can not only be reliably counted but with an
9 unexpectedly low coefficient of variation across many different incisors.

11 **Materials and methods**

12 **Ethical compliance**

13 All procedures involving animals were reviewed and approved by the IACUC committee at the University
14 of Michigan (UCUCA).

15 **Sample preparation:** Eighteen 7-week-old C57BL/6 wild type mice were anesthetized with isoflurane
16 and perfused for 20 min at room temperature with 4% paraformaldehyde in PBS (135 mM NaCl, 2.7 mM
17 KCl, 4.3 mM Na_2HPO_4 , 1.4 mM $\text{Na}_2\text{H}_2\text{-PO}_4$; pH 7.3). Hemi-mandibles were dissected from the head,
18 cleaned of muscle and soft tissues, and the bone covering the labial side of the incisors was chipped
19 away using dental tools. The hemi-mandibles were placed in small glass screw-top vials containing fresh
20 fixative and rotated overnight at 4°C. The hemi-mandibles were washed for another day at 4°C on the
21 rotator in several changes of PBS (pH 7.3), then dehydrated at room temperature in a graded series of
22 acetone, infiltrated for 5 days in dilute then pure Epon 812 substitute, embedded in rectangular silicone
23 molds and cured for 48 h at 60°C. Polymerized Epon blocks containing the embedded hemi-mandibles
24 were trimmed with a coarse rotary diamond wheel on a Model 650 Low Speed Diamond Wheel Saw
25 (South Bay Technology, San Clemente, CA, USA). Small 1-mm wide transverse (cross sectional) segments
26 of each mandibular incisor were then cut out with a fine diamond blade (0.15 mm) at a site located 8
27 mm from the apical end of along a plane that was perpendicular (normal) to the curving labial surface
28 (Level 8 section face, illustrated in Figure 2 of (Hu et al., 2011)). A group of 1-mm wide segments were
29 placed with the incisal aspect of the enamel layer face down in 25-mm diameter SeriForm mounting
30 cups (Struers, Ballerup, Denmark) and castolite AC plastic (Woodstock, IL, USA) was added and
31 polymerized overnight at room temperature. The Seriform blocks were polished with successively finer

1 grades (400, 600, and 800) of silicone carbide paper (South Bay Technology) followed by 16 h of
2 polishing with 1.0 μm alumina abrasive on a Syntron vibrating polisher. The polished block surfaces were
3 cleaned by sonication, the enamel surfaces etched and rapidly washed in liberal amount of distilled
4 water 3 times for 15 seconds each with 0.1% nitric acid and air-dried. The final surfaces were coated
5 with a thin layer of carbon.

6 **Backscatter electron imaging (BEI) and construction of enamel layer photo montages:** The enamel
7 layer covering the labial side of each incisor segment was identified and photographed at low
8 magnification (x200) as a single image at 25 kV using a Hitachi S-3000N variable pressure scanning
9 electron microscope in the backscatter mode (Fig. 1, panel A). Then, starting in the region of the mesial
10 cementoenamel junction a series of overlapping high magnification (x800) images were taken across the
11 entire face of the enamel layer from the lateral to the mesial cementoenamel junction (Fig. 1, panel B).
12 This process was repeated for enamel samples prepared from the right mandibular incisors of 18 mice.
13 In addition, the enamel layer covering the left mandibular incisors from 6 mice were also photographed.
14 Each group of 9-12 overlapping high magnification images of the enamel layer on each incisor was
15 placed into separate layers in a single large Photoshop file and aligned to recreate a large continuous
16 image of the entire enamel layer on each incisor (Fig. 1, panel B). The completed montages were
17 assessed for accuracy of high magnification alignments by comparing them against the single low
18 magnification images initially taken of the enamel layer on each incisor. A final merged image was
19 created, cropped to touch the surface of the enamel layer just lingual to the lateral cementoenamel
20 junction and enamel surface at the point of maximum convexity along the labial surface and either the
21 dentin or enamel surface at the mesial side (which ever projected the most), then saved in TIF format
22 for each montage.

23 **Color coding of enamel rods and quantitative analyses using ImageJ:** A four color coding scheme was
24 used to assign enamel rods into various groupings depending upon their regional location within the
25 enamel layer. These were BLACK for oval rod profiles within the inner enamel layer having a tilt pointed
26 toward the mesial cementoenamel junction, RED for oval rod profiles within the inner enamel layer
27 having a tilt pointed toward the lateral cementoenamel junction, BLUE for diamond-shaped rod profiles
28 forming the outer enamel layer, and MAGENTA for disorganized rod profiles located near the mesial and
29 lateral cementoenamel junctions (Moinichen et al., 1996) (Fig. 1, panels B and C). To do this, the TIF file
30 that contained the montaged image of the entire enamel layer on each incisor was brought into
31 Photoshop and four new imaging layers were created, one for each color. Working at about x300
32 enlargement, the sectioned profiles of the enamel rods were outlined and filled with the appropriate

1 color for each category on its appropriate image layer. When completed, an all color images overlaid on
2 the original montage could be saved by layer merging for illustration purposes or a color map for each
3 enamel rod grouping could be saved individually for quantitative analyses in ImageJ
4 (<https://imagej.nih.gov/ij/>). Single color maps representing the locations of enamel rod profiles in the
5 inner enamel layer having either a mesial or a lateral tilt were brought into ImageJ, converted to an 8-bit
6 greyscale image and a threshold was defined which best matched the outline of every rod profile in the
7 color map (in this case black or red). Starting near the central aspect of the enamel layer, a single row of
8 enamel rod profiles was identified and outlined with an irregular polygon from its lateral to mesial sides.
9 The “Analyze Particles...” function with “Show Outlines” was used to compute the profile area, centroid,
10 long and short Feret diameters and Feret angle for each rod profile contained within the polygonal
11 outline. The results were copied to Microsoft Excel and sorted by X-axis coordinate position of the
12 centroid, and the results checked for correct sequencing of rod profiles from lateral to mesial endpoints
13 by comparison to the outlines created by ImageJ following each particle count. Data were coded by
14 mouse ID (1-18), incisor ID (right or left), tooth ID (1-24), row tilt (mesial or lateral; 1 or 2), row ID (1-
15 max), and rod profile ID (1-max). From these raw data, the distance between rod profiles forming the
16 row (distance between x- and y-coordinates of centroids in sequence across the row) was computed
17 using the standard formula in coordinate geometry: $\text{distance} = \text{SQRT}((X_2 - X_1)^2 + (Y_2 - Y_1)^2)$. A second MS
18 Excel file was created for each incisor containing summary data for each row of rod profiles forming the
19 inner enamel layer in this tooth. This file included mouse, incisor, tooth, row and tilt identifiers as well as
20 summary variables defining number of rods per row (RPR), the coordinate locations of the lateral
21 endpoint, midpoint and mesial endpoint and their linear distances from the DEJ relative to a line drawn
22 perpendicular to the DEJ, length of row as sum of inter-coordinate centroid distances, and average
23 profile area, average long and short Feret diameters, and average Feret angle across all rod profiles
24 forming each row. The angle function in ImageJ computes angles relative to the horizontal image plane,
25 and in a counterclockwise direction with 0° in a 3 o’clock position (to the mesial side in the case of this
26 study) and 90° in the noon position. All raw data were collected in pixel units and converted afterwards
27 to μm as required using appropriate “pixels per micrometer” scaling factors (pixels/pixels per μm). The
28 x- and y-coordinate locations of the centroids of rod profiles in each map were also converted from
29 “imaging (real world) coordinates” to “normalized (virtual) coordinates” using a min/max function to
30 identify the boundaries of a rectangle that best fit the outer boundaries of the enamel layer in each
31 coordinate map. These min/max x- and y-coordinates could then be used to express rod profile locations
32 as a value ranging from a minimum of 0.0 to a maximum of 1.0 in both x and y directions. The color
33 maps constructed for rod profiles located in the outer enamel layer and near the cemento-enamel

1 junctions were processed in a similar fashion except that it was impossible to assign rod profiles in these
2 regions to any row arrangement. A nearest neighbor plugin for ImageJ therefore was used to determine
3 inter-centroid distances between rod profiles in these regions
4 ([https://icme.hpc.msstate.edu/mediawiki/index.php/Nearest_Neighbor_Distances_Calculation_with_Im](https://icme.hpc.msstate.edu/mediawiki/index.php/Nearest_Neighbor_Distances_Calculation_with_ImageJ)
5 [ageJ](https://icme.hpc.msstate.edu/mediawiki/index.php/Nearest_Neighbor_Distances_Calculation_with_ImageJ)). All other variables and coding schemes were the same as described above. Data were loaded from
6 Excel files into Version 13 of Statistica for Windows for graphing and statistical analyses
7 (<https://www.tibco.com/products/tibco-statistica>). Angle data was analyzed and graphed using Version
8 12 of NCSST for Windows (<https://www.ncss.com/software/ncss/>). A total number of 173,598 enamel rod
9 profiles from 24 incisors of 18 mice were analyzed in this study.

11 Results

12 Features of Gross Enamel Organization in Cross (Transverse) Sections of Mouse Incisors

13 The 2-dimensional organization of rod and interrod enamel in rat and mouse incisor enamel has been
14 described in detail by several researchers, e.g., (Warshawsky, 1971; Risnes, 1979; Moinichen et al.,
15 1996), and this classic organization is clearly discernable in medium resolution back scatter scanning
16 electron microscopic images (BEI) (Fig. 1). Briefly, mouse and rat incisor enamel consists two thin and
17 two thicker layers stacked on top of one another from the DEJ to the outer surface. These are: (1) the
18 innermost initial layer containing only a thin coat of interrod-type enamel which ameloblast create at
19 the start of amelogenesis (not visible in Fig. 1), (2) an inner enamel layer containing a long portion of
20 rods angled incisally and arranged in several sequential alternating sheets (rows) of rods traveling from
21 near the DEJ outward in either a mesial or a lateral direction toward the surface along with associated
22 interrod enamel, (3) an outer enamel layer containing a short portion of the rods all angled in an incisal
23 direction sloping towards the enamel surface with associated interrod enamel, and (4) the final enamel
24 layer also composed of only a thin coat of interrod-type enamel which ameloblasts produce to
25 terminate the appositional growth phase of amelogenesis (somewhat visible in Fig. 1). Quantitative
26 analyses of cross sections from 24 mandibular mouse incisors indicated that on average enamel layer
27 was $121 \pm 2.7 \mu\text{m}$ thick at the point of maximum convexity along the central labial side (Table). A cross
28 section of the enamel layer on average contained a total of $7,233 \pm 575$ identifiable rod profiles of which
29 70% (~5,000) were associated with the inner enamel layer (Fig. 1, black and red ovals), 27% (~2,000)
30 with the outer enamel layer (Fig. 1, blue ovals), and 3% (~200) with regions abutting the cemento-enamel
31 junctions (Fig. 1, magenta ovals) (summarized in Table). The $5,096 \pm 395$ rod profiles forming the inner

1 enamel layer were gathered into 124 ± 15 rows split equally by tilt angle (Table). Unexpectedly, a slight
2 but significantly higher number of rod profiles having a mesial tilt were counted compared to rod
3 profiles having a lateral tilt ($2,687 \pm 232$, $N= 64,480$ versus $2,409 \pm 204$, $N= 57,815$; Table).

4 **Rod Angulations Relative to Plane of Section Across the Enamel Layer**

5 The most prominent feature of rodent incisor enamel in cross section is the repetitive alternating
6 angulations to rod profiles across the thickness and breadth of the inner enamel layer (Fig. 1, panels B
7 and C, black and red ovals). In any given incisor, the angle at which rod profiles appeared tilted toward
8 the mesial side or the lateral side seemed similar at any given location vertically across the thickness of
9 the inner enamel layer, but there was a noticeable increase in angulation of all rod profiles progressing
10 from the lateral side to the mesial side of the enamel layer (Figs. 1 and 2). Rod profiles having a mesial
11 tilt showed the largest linear increase compared to rod profiles having a lateral tilt, which showed only
12 modest increases from lateral to mesial side (Figs. 2-3). This resulted in the impression that rod profiles
13 having a lateral tilt in section were more horizontal in the lateral region (region 1) and more vertical in
14 the mesial region (region 4) whereas rod profiles having a mesial tilt were more vertical in the lateral
15 region and near horizontal at a much higher angle in the mesial region (essentially inverted mirror
16 images of each other) (Figs. 2 and 4A). Also, on any given incisor and any region of the enamel layer, the
17 tilt angle showed considerable local variation within the same row, especially in the case of rows having
18 a lateral tilt (Fig. 3). Most of these variations were smoothed out when computed over all 24 incisors
19 analyzed in this study (Fig. 2, panels C and D for 1 incisor compared to Fig. 4A for all incisors).

20 In global terms, the angulation grand mean for rod profiles having a mesial tilt in 24 incisors was
21 $104.0^\circ \pm 34.2^\circ$ while rod profiles having a lateral tilt was $48.6^\circ \pm 25.2^\circ$ (Fig. 4B). Rod profiles having a
22 mesial tilt showed a mean angle of $58.4^\circ \pm 12.5^\circ$ in the lateral region (region 1) and a mean angle of
23 $147.0^\circ \pm 14.1^\circ$ in the mesial region (region 4) of the enamel layer (Fig. 4B) whereas rod profiles having a
24 lateral tilt show a mean angle of $29.9^\circ \pm 52.8^\circ$ in the lateral region and a mean angle of $75.6^\circ \pm 13.5^\circ$ in
25 the mesial region (Fig. 4B). This resulted in a progressive lateral-to-mesial regional change in angulation
26 of about 30° per region for a total of near 90° overall for rod profiles having a mesial tilt but only a 15°
27 step change per region and a 45° change overall, or one-half, for rod profiles having a lateral tilt (Fig.
28 4B).

29 Similar regional changes in rod profile angulation from lateral to mesial sides of the enamel layer
30 were also detected for the diamond-shaped rod profiles forming the outer enamel layer and the
31 irregularly elongated and tilted rod profiles found near the lateral and mesial cemento-enamel junctions

1 (Figs. 5-6). The changes in rod profile angulation from lateral to mesial regions of the outer enamel layer
2 and features of row angulation distributions across a given region or relative to enamel thickness
3 resembled changes observed for rod profiles having a mesial tilt within the inner enamel layer with the
4 exception that the angle changes per region were progressively larger per regional step and the total
5 change in angle from lateral to mesial was greater in the outer enamel layer compared to the inner
6 enamel layer (Fig. 5, panel B and Fig. 6A compared to Fig. 2, panels B and C and Fig. 4A; Fig. 5, panel C
7 compared to Fig. 3B top right; Fig. 6B compared to Fig. 4B). In global terms, the angulation grand mean
8 for rod profile forming the outer enamel layer in 24 mandibular mouse incisors was $69.5^\circ \pm 47.4^\circ$ and
9 $101.0^\circ \pm 43.9^\circ$ for rod profiles positioned near the mesial and lateral CEJ. In both cases, deviations in
10 angulation were very high in the lateral region especially for rod profiles near the CEJ which showed
11 considerable variation in angles relative to enamel thickness (Fig. 5, panel D and Fig. 6B).

12 **Rod Angulations Relative to the DEJ**

13 A somewhat different impression of enamel rod profile angulations and their changes from lateral to
14 mesial sides of the enamel layer was obtained when the imaging plane was aligned parallel to the DEJ
15 prior to making the angle measurements (Fig. 1, panel C; Fig. 7). One difference was that rod profile
16 angulations at the lateral side of the enamel layer appeared larger, while those at the mesial side
17 appeared reduced compared to measurements made relative to the plane of section (Fig. 7). This
18 resulted in greatly reduced changes in absolute angles progressively from lateral to mesial sides across
19 the enamel layer. Second, rod profiles within the inner enamel layer having a mesial tilt showed only a
20 modest increase in angulation from lateral to mesial sides, whereas rod profiles having a lateral tilt
21 showed little change, then a decrease in rod profile angulation approaching the mesial side of the inner
22 enamel layer (Fig. 7). Rod profiles forming the outer enamel layer and those located near the
23 cementoenamel junctions show similar trends for increasing angulations progressing from lateral to
24 mesial sides of the enamel layer, but only about one-half the absolute change in angulation compared to
25 measurements made relative to plane of section (Fig. 7)

26 **Angulation Changes Between Alternating Rows**

27 The alternating mesial and lateral tilts of rod profiles within the inner enamel layer creates two angles
28 that can be quantified. One is the simple angle difference between sequential rows, or decussation
29 angle (Moinichen et al., 1996) (Fig. 8A). This angle can be computed from grand means (Fig. 4B) or from
30 actual measurements of angles difference on a row-by-row basis (e.g., Figs. 3 and 7). Results from these
31 angle measurements are surprisingly consistent except for an underestimate of angle difference in the

1 lateral region of the inner enamel layer based upon grand means (Fig. 8A, region 1). The trend is for a
2 gradually increase in decussation angle between alternating rows until the mesial side of the inner
3 enamel layer, where the angle difference increases sharply (Fig. 8A). The second angle created when
4 rows of opposite tilts cross one another is the wide angle created where the two rows abut, herein
5 termed the alternating interrow angle (Fig. 8B). This angle can be measured either as a transition from
6 rows having a mesial tilt to rows having a lateral tilt (Fig. 8B, black-to-red with angle open to lateral side)
7 or between rows having a lateral tilt to rows having a mesial tilt (Fig. 8B, red-to-black with angle open to
8 mesial side). The alternating inter-row angle was consistently slightly higher for lateral-to-mesial row tilt
9 transitions (not significant), but in both cases the angle decreased from a maximum near 135° in region
10 2 (mid lateral) to a minimum near 110° in region 4 (mesial) in progressing from the lateral to mesial
11 sides of the inner enamel layer (Fig. 8B). These results suggest that measurements of angle differences
12 between rows are fairly independent of plane of section and tooth curvature (i.e., this parameter is row
13 dependent rather than plane of section or alignment dependent).

14 **Spacing of Rods Within the Enamel Layer**

15 The last feature of gross 2D arrangement of enamel rods examined in cross sections was the distance
16 between adjacent rod profiles forming rows within the inner enamel layer and, since they are not
17 arranged in clearly definable rows, the nearest neighbor distances between rod profiles forming the
18 outer enamel layer and those positioned near the cemento-enamel junctions (Fig. 9). The side-by-side
19 spacing of enamel rod profiles across rows having a mesial tilt showed a gradual compression
20 progressing from lateral to mesial sides of the inner enamel layer (Fig. 9). A similar trend for shortening
21 of the between rod profile spacing was seen in rows having a lateral tilt, but this occurred only between
22 region 1 (lateral) and region 2 (mid lateral). There was no change in the between rod profile spacing
23 from region 2 (mid lateral) to region 3 (central labial), but the spacing distance between rod profiles
24 increased by almost 2-fold in moving from the region 3 (central labial) to region 4 (mesial) of the inner
25 enamel layer (Fig. 9). Rod profiles forming the outer enamel layer were more tightly packed together
26 compared to rod profiles present within the inner enamel layer, which thereby allowed ~30% of all
27 enamel profiles (Table) to be packed into 20% of the cross-sectional area of the enamel layer (Fig. 1 and
28 Table). The outer enamel rod profiles showed the same trend as rod profiles in the inner enamel layer to
29 become more closely spaced between the lateral and central regions of the outer enamel layer (regions
30 1-3) followed by an increase in spacing in the mesial region (Fig. 9). Rod profiles located near the lateral
31 and mesial cemento-enamel junctions showed only slight differences in their nearest neighbor distances
32 (Fig. 10). They were more tightly packed together compared to rod profiles forming the inner enamel

1 layer but more dispersed compared to rod profiles forming the outer enamel layer (compare Fig. 10 to
2 Fig. 9). We found no evidence for any major change in packing density of the enamel rods relative to
3 enamel thickness, only a significant difference relative to regional division of the enamel layer.

4 5 **Discussion**

6 It was initially anticipated that attempts to count every enamel rod profile present in cross sections cut
7 from mouse mandibular incisors would prove very difficult to accomplish because of uncertainties at
8 many sites in distinguishing clearly the boundaries of rod profiles from their surrounding interrod
9 material. The most problematic sites include where the innermost ends of the enamel rods are located
10 in close proximity to the DEJ, the boundary region where the inner enamel portions of rods transition
11 into smaller and more diamond-shaped outer enamel portions (Warshawsky and Smith, 1971), and
12 where the outer enamel portions of the rods terminate near the enamel surface (Fig. 1, panel B). Enamel
13 rods also appear disorganized and their outlines obscure in areas approaching the cemento-enamel
14 junctions at the mesial and lateral sides of the enamel layer (Moinichen et al., 1996). As it turned out,
15 defining boundaries of rod profiles and counting them was not a major obstacle (Table). What proved
16 the most problematic was the technical issue of obtaining high clarity etchings of polished tooth slices.
17 This proved difficult to control and often repeat polishing and etching of tooth slices were required to
18 obtain the best imaging of the exposed enamel rod profiles. Both standard mode and backscattered
19 mode SEM were acceptable for creating high magnification montage maps of the enamel layer but
20 interrod material was more prominent, and caused more interpretive interference in the former and
21 this was the reason why the latter approach was chosen as the method of choice for this investigation.

22 All past reports of enamel rod distributions in cross sections of rodent incisor enamel have been
23 qualitative in nature and focused on features such as enamel thickness, general organization of rows of
24 rods within the inner enamel layer, or various angles at which the decussating enamel rods cross one
25 another or are tilted relative to the plane of eruption, the outer enamel layer, and/or the enamel
26 surface, e.g., (Warshawsky, 1971; Jodaikin et al., 1984; Moinichen et al., 1996). Moinichen et al. (1996)
27 published one of the most detailed and informative investigations about the 2D organization of the
28 enamel layer in mouse incisor. These workers did not attempt to quantify the number of enamel rod
29 profiles cut open in cross sections either globally or on a regional basis, but they noted several
30 important details about the structural arrangement of enamel rods in mouse incisor enamel pertinent to
31 findings in this study. **1. Enamel thickness.** Moinichen et al. (1996) reported that enamel thickness in the

1 central labial region was 95 μm on the erupted portion of mandibular incisors from 5-week-old Balb/c
2 albino mice. We found enamel thickness was $121 \pm 2.7 \mu\text{m}$ in pre-eruptive enamel near the gingival
3 margin in 7-week-old C57BL/6 pigmented mice (Table). There are several possible reasons for this 20%
4 discrepancy in thickness measurements including strain differences (Li et al., 2013), but the more likely
5 explanation is related to age and site of sampling for imaging. In pre-eruptive and early post eruptive
6 rodent incisors, the diameter of the developing tooth at its incisal end is always smaller than the part of
7 the tooth buried more apically (Sehic et al., 2009). This is due to growth changes in diameter and length
8 of the incisors which take time to stabilize. We found in preliminary studies that these growth changes
9 in size take around 7 weeks to terminate. This is confirmed by a later report from the same research
10 group noted above that enamel thickness in adult wild type mice (> 2 months in age) was $128 \pm 8 \mu\text{m}$
11 (Risnes et al., 2005), almost identical to the thickness value we obtained. **2. Incisal Tilt Angle of Enamel**
12 **Rods.** The enamel rods in rodent incisors do not travel in straight lines from the DEJ to the surface but
13 are all angled in a forward (incisal) direction, which is why they appear within the inner enamel layer in
14 profile as elongated ovals in cross sections. The incisal tilt angle is not fixed to one specific value but
15 varies by species (e.g., rat versus mouse), tooth type (maxillary versus mandibular incisor) and location
16 within the enamel layer (outer enamel layer versus inner enamel layer). Moinichen et al. (1996)
17 reported that in mandibular mouse incisors the alternating rows of rods forming the inner enamel layer
18 are tilted incisally by 45° relative to the DEJ whereas the outer enamel portions of the rods are angled
19 more broadly at 88° thereby creating an angle of 12° to the enamel surface. In this study we used
20 sections cut only in the cross-sectional plane and therefore could not estimate the incisal tilt angle. **3.**
21 **Rod Decussation Angle.** There has been considerable disagreement in the literature regarding the angle
22 at which the alternating rows of rods cross one another traveling in either a mesial or lateral direction
23 across the thickness of the inner enamel layer in rat and mouse incisors, from as little as 30° (Moinichen
24 et al., 1996) to as much as 90° (Warshawsky, 1971). As with rod incisal tilt angle, differences by species
25 and tooth type have been noted for decussation angles in mandibular mouse incisors (von Koenigswald,
26 1985; Moinichen et al., 1996; Martin, 1999; Vieytes et al., 2007), but by far the greatest differences were
27 reported by Moinichen et al. (1996) relative to positional location of rows across the thickness of the
28 inner enamel layer, that is, a decussation angle in mandibular mouse incisors of 30° near the DEJ, an
29 angle of 60° in the middle portion of the inner enamel layer, and a decussation angle of 80° near the
30 boundary of inner and outer enamel layers. The average decussation angle observed in this study based
31 on grand means for row tilts (Figs. 4B and 8A) was comparable to a grand mean that can be computed
32 from the range of decussation angles reported by Moinichen et al. (1996) ($104^\circ - 49^\circ = 55^\circ$ versus circular
33 mean of $30^\circ + 60^\circ + 80^\circ = 57^\circ$). We were unable, however, to find a trend for a 30° to 80° decussation angle

1 increase across the thickness of the inner enamel layer relative to either single incisors (Fig. 2 C and D, y-
2 axis of graphs) or in data pooled from multiple incisors (Fig. 5, y-axis of paired graphs). Instead we found
3 that the greatest change in rod tilt angulations, and computed decussation angle relative to the two
4 opposing rod tilts within the 2D plane of a cross section, occurred in the x-axis direction (lateral-to-
5 mesial side of the enamel layer) rather than in the y-axis direction (thickness) especially relative to rows
6 having a mesial tilt (Figs. 2-4 and 7). Of interest in this study was the finding that increases in rod profile
7 angulations from lateral-to-mesial side of the enamel layer (the direction rows of rods are organized
8 into), and to a lesser extent from DEJ-to-surface, did not occur in a smooth, regular fashion but the
9 transitions were often noisy, with increases and decreases in tilt angles intermixed at certain local sites
10 even within the same row (e.g., Fig. 3). Increases in rod angulations were apparent only by computing
11 grand means with a broader partition of the enamel layer (e.g., divisions by region; Figs. 2-4). Of interest
12 was the additional finding that the increase in rod angulation from lateral to mesial side of the enamel
13 layer also applied to the diamond-shaped outer enamel portions of the enamel rods (Figs. 5-7). In global
14 terms, the change in angulation of tilt of the outer enamel portion of the enamel rods resembled
15 changes detected for rod profiles having a mesial tilt within the inner enamel layer, but in regional terms
16 the grand means computed for rod angulation in the lateral one-half of the enamel layer (regions 1 and
17 2) resembled grand means computed for rod profiles having a lateral tilt whereas the means resembled
18 rod profiles having a mesial tilt in the mesial one-half of the enamel layer (regions 3 and 4; Figs. 4-7). To
19 the knowledge of the authors, these characteristics of rod profile angulation changes within the outer
20 enamel layer have not previously be reported including the study done by Moinichen et al. (1996) who
21 focused on differences in the incisal tilt angle for the outer enamel portions of rods which we did not
22 investigate in this study. **4. Arrangement of Enamel Rods Near the Cementoenamel Junctions.**
23 Moinichen et al. (1996) are among few investigators that have drawn attention to the unusual
24 appearance and arrangements of enamel rods located at sites near the lateral and mesial
25 cementoenamel junctions in rat and mouse incisors. Here row arrangements are obscure, rod tilts are
26 disorderly, organization of rods into inner and outer enamel portions is difficult to define and interrod
27 type enamel appears more prominent (Figs. 1, 5, 7). Of interest in this study were the findings that mean
28 tilt angle of these disorganized rods followed the same regional trend to be greater at the mesial side
29 than at the lateral side of the enamel layer, and that almost 5 times more rod profiles per cross section
30 were detected mesially than laterally (Fig. 7, N values), presumably in part reflecting the fact that the
31 whole enamel layer is thinnest near the lateral cementoenamel junction (Fig. 1). The cementoenamel
32 junctions are the last sites to develop during the secretory stage, and the disorganization of rods formed
33 in these areas may reflect a barrier function that occurs by ameloblasts to allow smoothing at the

1 outermost edges of the enamel layer that would otherwise show a step-like ragged arrangement
2 relative to terminations of rows having alternating tilts. **5. Rod spacing.** The packing density of enamel
3 rods within the enamel layer has not been investigated to any extent by past investigators. Figure 9
4 shows clearly that, like rod tilt angles, there is regional variation in the way enamel rods are packed
5 together but with opposite trends. That is, within the inner and outer enamel layers the rods are spaced
6 farther apart in the extreme lateral region (region 1) than in the central labial region (region 3). For rod
7 profiles within the inner enamel layer having a mesial tilt there is further shortening of the distance
8 between neighbors from the central labial region to the mesial region (region 4) of the enamel layer,
9 whereas for rod profiles having a lateral tilt and rod profiles forming the outer enamel layer neighboring
10 rods spread farther apart from one another (Fig. 9). There appears on a regional basis comparing Figure
11 7 to Figure 9 an inverse correlation between rod tilt angle relative to the DEJ and rod spacing at all sites
12 within the enamel layer. If the angle increases from one region to the next the rod spacing decreases, if
13 the angle stays unchanged so does the rod spacing whereas if the rod angle decreases the rod spacing
14 increases (Figs. 7 and 9). This could reflect structural concessions in that the enamel is highly curved
15 from lateral to mesial sides along the DEJ and varies in thickness from lateral to mesial sides. The finding
16 of the highest density of rods concentrated in the central labial region (region 3) could also comprise a
17 structural feature that allows the incisor tip to maintain a shovel-shape, with the sharp tip positioned in
18 the central labial plane (von Koenigswald, 1985; Kuang-Hsien Hu et al., 2014).

19 The global arrangement of enamel rods within the enamel layer of rodent incisors is clearly
20 complex and has proven difficult to conceptualize in histological sections. One aspect of the global
21 arrangement of enamel rods that past investigators have not fully taken into account is the mosaic
22 nature of rod arrangements in terms of time and space. That is, while there is a high degree of
23 symmetry and continuity to the way in which enamel rods fill the enamel layer, the packing of these
24 enamel rods as seen in a typical cross section of mature rodent incisor enamel represents a composite
25 image built up over time to create its final amalgamated form in 3D space (Fig. 10) (Smith and
26 Warshawsky, 1976). In terms of space, rod profiles seen near the DEJ represent the starting point of
27 rods projecting forward almost in their entirety out of the plane of section while rod profiles situated
28 the middle of the enamel layer represent rods cut at their midpoints with half the rod projecting
29 backwards into block of tissue and the other half projecting forwards out of the plane of section. Rod
30 profiles seen near the surface in the cross section represent the endpoints of rods projecting almost in
31 their entirety backwards into the block (Fig. 10). Hence, the thickness of the enamel layer, which
32 develops over the duration of the secretory stage by an appositional growth process, requires the

1 coordinated efforts of all those ameloblasts needed to maintain continuity across the boundaries
2 delineated between the lateral and mesial cemento enamel junctions (Smith and Warshawsky, 1976).
3 This is one of the main reasons for wanting to know how many rod profiles are present within a
4 representative cross section of rodent incisor enamel, as it puts into perspective the basic unit (cohort)
5 of ameloblasts needed to renew the enamel layer over time (Smith and Warshawsky, 1977). This
6 investigation has suggested that this involves the participation of approximately 7,200 ameloblasts per
7 renewal cycle (Table). There are two additional implications of this step-like development of enamel
8 rods relative to the longitudinal axis of the incisor. The first is that ameloblasts located at the enamel
9 surface at the end of the secretory stage have no formative relationship to 99.9% of the enamel rods
10 situated vertically between them and the DEJ (as would be seen a cross section of the incisor). The
11 enamel rods they have produced all project BACKWARDS (apically) from the site where they are
12 currently located (Fig. 10). The second implication is that throughout the maturation stage a given group
13 of ameloblasts is assisting the final mineralization in the vertical plane of portions of thousands of
14 enamel rods they did not secrete.

15 There is a second developmental axis in rodent incisor enamel formation besides the one
16 associated with appositional growth (progressive development of enamel thickness from DEJ to surface).
17 This also requires time and space to develop fully and involves the spread of a wave of differentiation
18 from the point of maximum convexity along the central labial aspect of the tooth (equivalent to the
19 incisal edge on a human incisor) in mesial and lateral directions until a termination point is reached at
20 what becomes the mesial and lateral cemento enamel junctions (equivalent to the cervical area on a
21 human incisor) (Fig. 10) (Smith and Warshawsky, 1976). It takes more time for the wave of
22 differentiation to terminate laterally than mesially thereby creating the side-to-side asymmetry typical
23 of rodent incisor enamel (Moinichen et al., 1996). It is prior to or during the movement of this wave that
24 the row arrangements with alternating rod tilts characteristic of the lamellar sheet arrangement of rods
25 forming the inner enamel layer are established (Smith and Warshawsky, 1976; Cox, 2013). It is
26 presumably the time delay between the start of formation of enamel in the central labial region and the
27 completion of the wave of ameloblast induction at the sites, which become the mesial and lateral
28 cemento enamel junctions, that ultimately creates the step-like pattern of rod arrangement in the
29 enamel layer.

30

31 **Acknowledgements**

1 This study was supported by NIDCR/NIH grant DE015846 (JC-CH) .

2 **Conflict of interest**

3 The authors declare no conflict of interest.

5 **Author contributions**

6 This study was designed principally by CES with contributions by JPS and JC-CH. The incisors were
7 prepared, sectioned, polished and BEI imaged by YH. JC-CH oversaw the growth and mating of mice.
8 Data analysis and crafting the first draft of the manuscript and figures was performed by CES. The
9 figures were modified by JPS. The manuscript was critically reviewed by JC-CH and JPS.

10 **References**

- 11 **Boyde A** 1967. The development of enamel structure. *Proc R Soc Med*, **60**, 923-8.
- 12 **Boyde A** 1969. Electron microscopic observations relating to the nature and development of prism
13 decussation in mammalian dental enamel. *Bull Group Int Rech Sci Stomatol*, **12**, 151-207.
- 14 **Boyde A** 1989. Enamel. In: OKSCHE, A. & VOLLRATH, L. (eds.) *Handbook of Microscopic Anatomy: Teeth*.
15 Berlin: Springer-Verlag.
- 16 **Cox BN** 2013. How the tooth got its stripes: patterning via strain-cued motility. *J R Soc Interface.*, **10**,
17 20130266.
- 18 **Habelitz S** 2015. Materials engineering by ameloblasts. *J Dent Res.*, **94**, 759-67.
- 19 **Hu Y, Hu JC, Smith CE, et al.** 2011. Kallikrein-related peptidase 4, matrix metalloproteinase 20, and the
20 maturation of murine and porcine enamel. *Eur J Oral Sci*, **119**, 217-25.
- 21 **Jernvall J, Thesleff I** 2012. Tooth shape formation and tooth renewal: evolving with the same signals.
22 *Development.*, **139**, 3487-97.
- 23 **Jodaikin A, Weiner S, Traub W** 1984. Enamel rod relations in the developing rat incisor. *J Ultrastruct Res*,
24 **89**, 324-32.

- 1 **Klein OD, Duverger O, Shaw W, et al.** 2017. Meeting report: a hard look at the state of enamel research.
2 *Int J Oral Sci.*, **9**, e3.
- 3 **Kuang-Hsien Hu J, Mushegyan V, Klein OD** 2014. On the cutting edge of organ renewal: Identification,
4 regulation, and evolution of incisor stem cells. *Genesis.*, **52**, 79-92.
- 5 **Li Y, Konicki WS, Wright JT, et al.** 2013. Mouse genetic background influences the dental phenotype.
6 *Cells Tissues Organs*, **198**, 448-56.
- 7 **Lyngstadaas SP, Moinichen CB, Risnes S** 1998. Crown morphology, enamel distribution, and enamel
8 structure in mouse molars. *Anatomical Record*, **250**, 268-80.
- 9 **Martin T** 1999. Evolution of incisor enamel microstructure in Theridomyidae (Rodentia). *J Ver Paleo*, **19**,
10 550-565.
- 11 **Moinichen CB, Lyngstadaas SP, Risnes S** 1996. Morphological characteristics of mouse incisor enamel. *J*
12 *Anat*, **189**, 325-33.
- 13 **Nishikawa S** 2017. Cytoskeleton, intercellular junctions, planar cell polarity, and cell movement in
14 amelogenesis. *J Oral Biosci*, **59**, 197-204.
- 15 **Peterkova R, Hovorakova M, Peterka M, et al.** 2014. Three-dimensional analysis of the early
16 development of the dentition. *Aust Dent J.*, **59**, 55-80.
- 17 **Pugach MK, Gibson CW** 2014. Analysis of enamel development using murine model systems:
18 approaches and limitations. *Front Physiol.*, **5**, 313.
- 19 **Renvoisé E, Michon F** 2014. An Evo-Devo perspective on ever-growing teeth in mammals and dental
20 stem cell maintenance. *Front Physiol.*, **5**.
- 21 **Risnes S** 1979. A scanning electron microscope study of aberrations in the prism pattern of rat incisor
22 inner enamel. *Am J Anat*, **154**, 419-36.
- 23 **Risnes S, Peterkova R, Lesot H** 2005. Distribution and structure of dental enamel in incisors of Tabby
24 mice. *Arch Oral Biol*, **50**, 181-4.
- 25 **Risnes S, Septier D, Deville De Periere D, et al.** 2002. TEM observations on the ameloblast/enamel
26 interface in the rat incisor. *Connect Tissue Res*, **43**, 496-504.

- 1 **Schour I, Massler M** 1949. The Teeth. In: FARRIS, E. J. & GRIFFITH JR., J. Q. (eds.) *The Rat in Laboratory*
2 *Investigation*. Philadelphia: Lippincott Co.
- 3 **Sehic A, Peterkova R, Lesot H, et al.** 2009. Distribution and structure of the initial dental enamel formed
4 in incisors of young wild-type and Tabby mice. *Eur J Oral Sci*, **117**, 644-54.
- 5 **Seidel K, Marangoni P, Tang C, et al.** 2017. Resolving stem and progenitor cells in the adult mouse
6 incisor through gene co-expression analysis. *Elife.*, **6**, e24712.
- 7 **Skobe Z** 2006. SEM evidence that one ameloblast secretes one keyhole-shaped enamel rod in monkey
8 teeth. *Eur J Oral Sci*, **114 Suppl 1**, 338-42; discussion 349-50, 382.
- 9 **Smith CE** 1998. Cellular and chemical events during enamel maturation. *Crit. Rev. Oral Biol. Med.*, **9**,
10 128-61.
- 11 **Smith CE, Nanci A** 1989. A method for sampling the stages of amelogenesis on mandibular rat incisors
12 using the molars as a reference for dissection. *Anat Rec*, **225**, 257-66.
- 13 **Smith CE, Warshawsky H** 1975. Cellular renewal in the enamel organ and the odontoblast layer of the
14 rat incisor as followed by radioautography using 3H-thymidine. *Anat. Rec.*, **183**, 523-61.
- 15 **Smith CE, Warshawsky H** 1976. Movement of entire cell populations during renewal of the rat incisor as
16 shown by radioautography after labeling with 3H-thymidine. The concept of a continuously
17 differentiating cross-sectional segment. (With an appendix on the development of the
18 periodontal ligament). *Am. J. Anat.*, **145**, 225-59.
- 19 **Smith CE, Warshawsky H** 1977. Quantitative analysis of cell turnover in the enamel organ of the rat
20 incisor. Evidence for ameloblast death immediately after enamel matrix secretion. *Anat. Rec.*,
21 **187**, 63-98.
- 22 **Vieytes EC, Morgan CC, Verzi DH** 2007. Adaptive diversity of incisor enamel microstructure in South
23 American burrowing rodents (family Ctenomyidae, Caviomorpha). *J Anat.*, **211**, 296-302.
- 24 **Von Koenigswald W** 1985. Evolutionary trends in the enamel of rodent incisors. In: LUCKETT, W. P. &
25 HARTENBERGER, J.-L. (eds.) *Evolutionary Relationships among Rodents: A Multidisciplinary*
26 *Analysis*. New York: Springer Science.

1 **Von Koenigswald W** 2004. Enamel Microstructure of Rodent Molars, Classification, and Parallelisms,
 2 with a Note on the Systematic Affiliation of the Enigmatic Eocene Rodent *Protoptychus*. *J*
 3 *Mamm Evol*, **11**, 127–142.

4 **Warshawsky H** 1971. A light and electron microscopic study of the nearly mature enamel of rat incisors.
 5 *Anat. Rec.*, **169**, 559-83.

6 **Warshawsky H, Smith CE** 1971. A three-dimensional reconstruction of the rods in rat maxillary incisor
 7 enamel. *Anat. Rec.*, **169**, 585-91.

8 **Yilmaz ED, Schneider GA, Swain MV** 2015. Influence of structural hierarchy on the fracture behaviour of
 9 tooth enamel. *Philos Trans A Math Phys Eng Sci.*, **373**, rsta.2014.0130.

13 **Table. Final Summary Data**

14	1. Enamel thickness	121 ± 2.7 µm
15	Inner enamel layer	100.0 ± 2.6 µm (83%)
16	Outer enamel layer	21.0 ± 2.1 µm (17%)
17	2. Total number of rod profiles in cross section	7,233 ± 575
18	Inner enamel layer =	5,096 ± 395 (70%)
19	Number with mesial tilt =	2,687 ± 232
20	Number with lateral tilt =	2,409 ± 204**
21	Outer enamel layer =	1,922 ± 191 (27%)
22	Sites near CEJs =	216 ± 56 (3%)
23	3. Per cross section:	
24	Total number of rows (inner enamel)	124 ± 15

1	Number with mesial tilt	62 ± 7
2	Number with lateral tilt	62 ± 9

3
4 Table. Final summary data for mandibular incisors cross section cut at
5 Level 8* (grand means ± standard deviation).

6 *Near gingival margin at labial aspect of incisor; N= 24 incisors from 18 mice

7 **p<0.0001)

8
9
10 **Legends to Figures**

11 **Figure 1. Orientation to the enamel layer and method employed for quantifying enamel rods in cross**
12 **sections.** Illustration of approach employed for making high magnification maps of the labial
13 side of mandibular mouse incisors from montaged BEI images and for color coding enamel rod
14 profiles by their regional distribution within the enamel layer: inner enamel layer with rod
15 profiles having a mesial (black) or lateral (red) tilt, outer enamel layer with rod profiles
16 appearing diamond-shaped (blue), and irregular rod profiles located near the lateral and mesial
17 cementoenamel junctions (CEJ) (magenta). Panel A, low magnification BEI image (x200, bar =
18 100 µm) of labial side of the mandibular mouse incisor showing location of enamel and dentin in
19 a typical cross section of the tooth. The cracks in the dentin are an artifact caused by air drying
20 the tissue slice. Panel B, a high-resolution map of the same tooth section shown in Panel A made
21 from BEI images photographed at x800 (bar = 50 µm) and montaged together to recreate the
22 whole enamel layer. The site for measuring enamel thickness and regional subdivisions of the
23 enamel layer are indicated. Panel C, some quantitative measurements of rod profile tilt angles
24 were made by cropping out areas so their edges were oriented parallel to the DEJ rather than
25 within the plane of the cross section (box, panel B).

26 **Figure 2. Example data for rod profile angles in the inner enamel layer measured in a single**
27 **mandibular mouse incisor.** Angle data from a single mandibular mouse incisor for rod profiles in
28 the inner enamel layer having a mesial tilt (black) or a lateral tilt (red). Panel A, color map for
29 rod profiles. The enamel layer is partitioned into 4 equally spaced regions from lateral (1) to

1 mesial (4) sides. Panel B, graph of rod profile tilt angle (y-axis) versus location across the face of
2 the cross section expressed as virtual coordinates (x-axis). The number of rod profiles plotted
3 from Panel A are indicated for each tilt (N=) as are schematic representations of the mean rod
4 profile tilts by the large ovals plotted for the lateral (1) and mesial (4) regions. Rod profiles
5 having a mesial tilt (black) show a linear increase in angulations from lateral to mesial sides
6 while rod profiles having a lateral tilt (red) increase initially from lateral to mid lateral regions (1
7 to 2) and only gradually thereafter (3 and 4). Panels C and D, distance weighted least squared 3D
8 surface plots of rod profile angulations (z-axis) relative to regional location (x-axis) and location
9 within the thickness of the enamel layer (y-axis) and row tilt (mesial tilt, C; lateral tilt, D). Data
10 values are overlaid to assist visualizing tooth profile outline relative to the more linear surface
11 plot. Some small variations in rod profile angle occur across the thickness of the enamel layer
12 (uniformity of color across the y-axis a given x-axis coordinate location) but the greatest change
13 in rod profile angle occurs relative to regional location across the face of the cross section
14 (change in color relative to x-axis).

15 **Figure 3. Scatter plots of tilt angle of rod profiles across rows and depth of the inner enamel layer in**
16 **the lateral (1), mid lateral (2), central labial (3), and mesial (4) regions of the inner enamel**
17 **layer on a single incisor.** Graphs from a single mandibular mouse incisor showing the
18 distribution of rod profile angles for rows having a mesial tilt (left side) or lateral tilt (right side)
19 relative to the mean circular angle (less than, brown; greater than, cyan) computed on a
20 regional basis (lateral, region 1; mid lateral, region 2, central labial, region 3; and mesial, region
21 4). Rod profile angles across different rows or across the thickness of the enamel layer are very
22 variable and show no clear pattern and less so for rows having a lateral tilt compared to those
23 having a mesial tilt where changes in the mean circular angle occur more dramatically between
24 regions. The central labial region (3) is the only part of the enamel layer showing some
25 similarities in the distributions of rod profile angles relative to the mean for the two rod tilt
26 categories. In the mesial region (4) rods profiles having a lateral tilt are more widely spaced
27 apart from one another compared to the other regions.

28 **Figure 4. 3D surface and circular plots of rod profile angles using pooled data from all incisors. 3D**
29 **surface plots of rod profile angles across the width and thickness of the inner enamel layer**
30 (panel A). Distance weighted least squared 3D surface plots of rod profile angles across the
31 entire inner enamel layer pooled from all mandibular mouse incisors examined in this study (z-
32 axis) plotted relative to regional location (x-axis) and location within the thickness of the enamel

1 layer (y-axis) separated by row tilt (mesial tilt, lateral tilt). These graphs, based on data from 24
2 incisors, bear a striking similarity to the results obtained from one incisor (Fig. 2, Panels C and D)
3 suggestive that the detected rod profile angle changes occur in a highly repetitive manner in
4 mouse incisor enamel (data from 1 tooth is representative of the pattern present in 24 teeth). In
5 this figure the trends across enamel thickness (y-axis) and regional location (x-axis) are merely
6 smoother and more uniform than in Figure 2. Circular plots of rod profile angles in the inner
7 enamel layer partitioned by region and by tilt (panel B). Circular plots of rod profile angles in the
8 inner enamel layer partitioned by region (Fig. 2, panel A) and by tilt (mesial, lateral) for all
9 mandibular mouse incisors. Measurements are in a counterclockwise direction from the 3:00
10 o'clock position (0°) with the lateral CEJ situated on the right side and mesial CEJ on the left side
11 of each circle. The four regions of the inner enamel layer are represented by color (1, red; 2,
12 blue; 3, green; 4, violet); points= counts, bars= relative number of observations per color, point
13 with line= mean circular direction (also indicated by numbers \pm circular standard deviation). The
14 mean profile tilt angle of rod profiles having a mesial tilt on average is roughly twice as large as
15 rod profiles having a lateral tilt. The regional means and the increase in profile angle from lateral
16 to mesial sides of the inner enamel layer also show this 2:1 difference for rod profiles having a
17 mesial tilt compared to those having a lateral tilt. (N= total number of rod profiles analyzed in
18 estimating grand means)

19 **Figure 5. Example data for rod profile angles in the outer enamel layer measured in a single**

20 **mandibular mouse incisor.** Angle data from a single mandibular mouse incisor for rod profiles
21 forming the outer enamel layer (blue) and those located near the mesial and lateral CEJ
22 (magenta). Panel A, color map for rod profiles. The enamel layer is partitioned into 4 equally
23 spaced regions (the same as in Fig. 2). Panel B, graph of rod profile tilt angle (y-axis) versus
24 location across the face of the cross section expressed as virtual coordinates (x-axis). The
25 number of rod profiles plotted from Panel A are indicated (N=), as is a schematic representation
26 of the mean rod profile tilt in the outer enamel layer by the diamonds plotted for the lateral (1)
27 and mesial (4) regions. Rod profiles forming the outer enamel layer (blue) show a linear increase
28 in angulations from lateral to mesial sides, while rod profiles situated near the CEJ are more
29 randomly arranged. Panel C, graph showing the distribution of rod profile angles in the outer
30 enamel layer of the central labial region (Panel A, region 3, blue) relative to the mean circular
31 angle (less than, brown; greater than, cyan). There is a general trend for rod profile angles to
32 increase in a mesial direction (with some irregularities) but no evidence for a similar change

1 relative to enamel thickness. Panel D, graph showing the distribution of rod profile angles near
2 the mesial CEJ (Panel A, region 4, magenta) relative to the mean circular angle (less than, brown;
3 greater than, cyan). Enamel rod profile at this site appear randomly tilted irrespective of
4 location.

5 **Figure 6. 3D surface and circular plots of rod profile angles across the width and thickness of the outer
6 enamel layer.**

7 3D surface plots for a single incisor compared to pooled data from all incisors
8 (panel A). Distance weighted least squared 3D surface plots of rod profile angles across the
9 entire outer enamel layer for one mandibular mouse incisor and for data pooled from all
10 mandibular mouse incisors examined in this study (z-axis) plotted relative to regional location (x-
11 axis) and location within the thickness of the enamel layer (y-axis). These graphs (based on 1
12 incisor and 24 incisors) bear a striking similarity to each other suggestive that the detected rod
13 profile angle changes occur in a highly repetitive manner in mouse incisor enamel (data from 1
14 tooth is representative of the pattern present in 24 teeth). Circular plots of rod profile angles
15 across the width and thickness of the outer enamel layer partitioned by region and for rod
16 profiles located near the mesial and lateral CEJ (panel B). Circular plots of rod profile angles in
17 the outer enamel layer and near the mesial and lateral CEJ partitioned by region (Fig. 5, panel A)
18 for all mandibular mouse incisors. Measurements are in a counterclockwise direction from the
19 3:00 o'clock position (0°) with the lateral CEJ situated on the right side and mesial CEJ on the left
20 side of each circle. The four regions of the inner enamel layer are represented by color (1, red; 2,
21 blue; 3, green; 4, violet); points= counts, bars= relative number of observations per color, point
22 with line= mean circular direction (also indicated by numbers \pm circular standard deviation). Rod
23 profile angles within the outer enamel layer increase by 4-fold from lateral to mesial sides of the
24 enamel layer, much greater than is seen for rods forming the inner enamel layer (Fig. 4B) or
25 positioned near the CEJ (right panel). (N= total number of rod profiles analyzed in estimating
grand means)

26 **Figure 7. Graphs summarizing rod profile angle relationships across the four regions of the enamel
27 layer as measured relative to the plane of section or to the DEJ.**

28 Graphs summarizing rod
29 profile angle relationships across the four regions of the enamel layer (1, lateral; 2, mid lateral,
30 3, central labial; 4, mesial) within the inner enamel layer (IE), the outer enamel layer (OE) and
31 near the CEJ as measured either within the plane of section (transverse) or relative to cropping
32 box positioned parallel to the DEJ. At the left and right sides of the graphs are BEI images of the
lateral and mesial regions (1 and 4) with example rod profiles having a mesial (black) or lateral

1 (red) tilt for orientation purposes. At the left side an image of a protractor is included for
2 reference. Data are from the right and left mandibular incisors of 6 mice (12 incisors total).
3 Number of rods analyzed, N= 50,000 relative to the DEJ and N= 92,500 relative to plane of
4 section. Angulation differences from lateral to mesial sides of a cross section are much less
5 pronounced for rod profiles forming the inner enamel layer when imaging fields are aligned
6 parallel to the DEJ prior to measurement. Angulation differences are relatively unchanged for
7 rod profiles forming the outer enamel layer and those located near the cemento-enamel
8 junctions irrespective of alignment method.

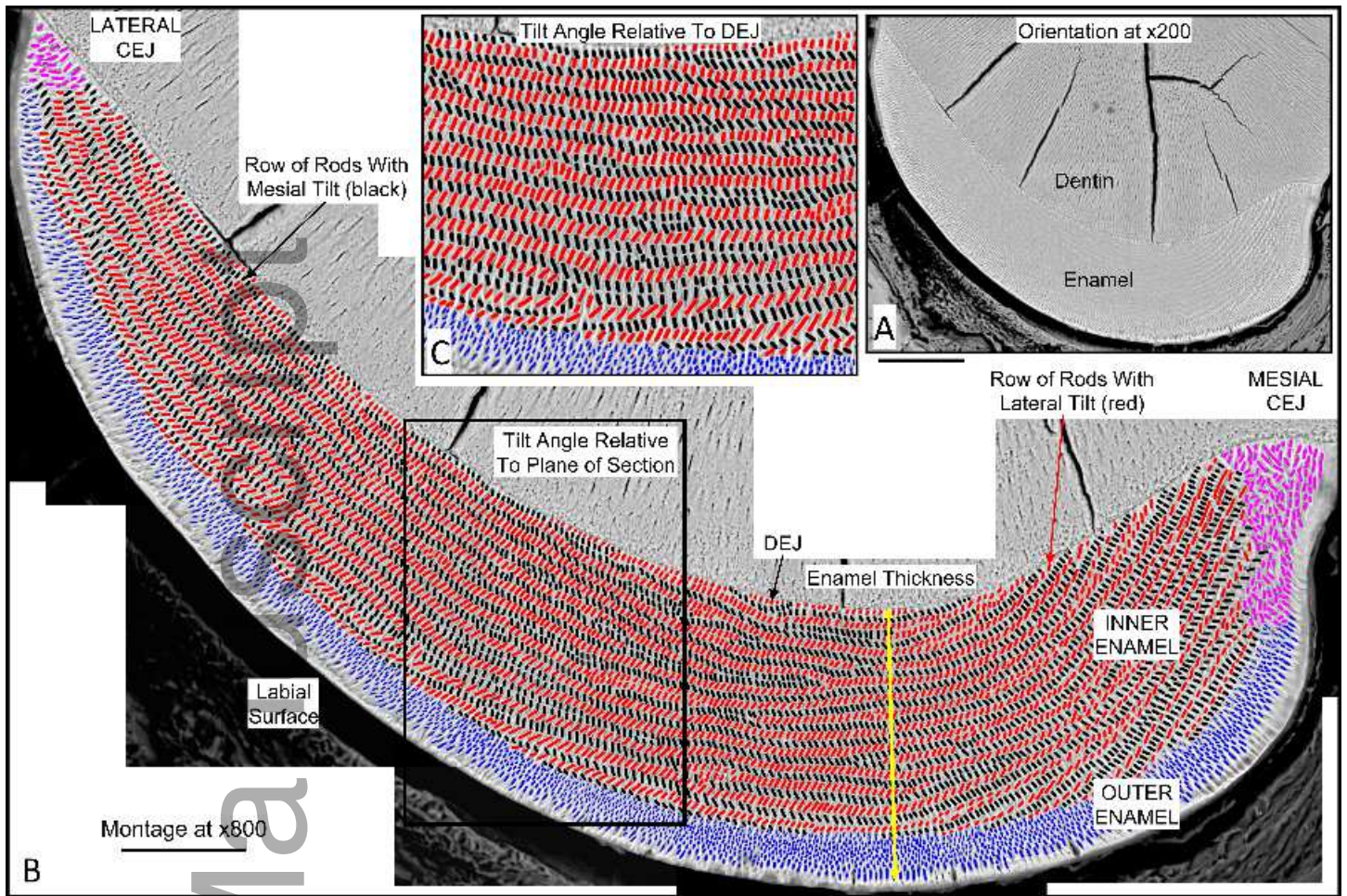
9 **Figure 8. Decussation and alternating inter-row angles.** Decussation angle between rows alternating
10 between mesial and lateral tilts computed from mean angles or as measured relative to the
11 plane of section or to the DEJ (panel A). Decussation angle between rows with alternating mesial
12 and lateral tilts measured across the four regions of the inner enamel layer (1, lateral; 2, mid
13 lateral, 3, central labial; 4, mesial). At the left side of the table is a small cropped area of the
14 inner enamel layer from a color map (black= mesial tilt; red= lateral tilt) illustrating with the
15 yellow lines the decussation angle (green arrow). Number of alternating rows analyzed, N=
16 2,974 from 24 mandibular incisors. These results suggest that measurements of the decussation
17 angle are independent of plane of section and tooth curvature (i.e., this variable is row
18 dependent rather than plane of section or alignment dependent). Considering the manner in
19 which row development occurs in the incisor (see Fig. 10), these data further suggest that the
20 decussation angle between rows with alternating tilts increases sharply as the wave of
21 differentiation spreads mesially from the central labial side of the tooth (region 3 to 4), but
22 decussation angle changes little as the wave spreads laterally (from region 3 to 2 then to region
23 1). Alternating inter-row angle measured across the four regions of the inner enamel layer
24 (panel B). Alternating inter-row angle measured across the four regions of the inner enamel
25 layer (1, lateral; 2, mid lateral, 3, central labial; 4, mesial). At the left side of the table is a small
26 cropped area of the inner enamel layer from a color map (black= mesial tilt; red= lateral tilt)
27 illustrating with the yellow lines the inter-row angle as the alternation from mesial (black) to
28 lateral (red) tilt or from lateral (red) to mesial (black) tilt (green arrows). Number of alternating
29 rows analyzed, N= 480 per tilt category from 12 mandibular incisors. There are no clear
30 differences between the red points and black points within the same region. As expected, the
31 inter-row angle is smallest in the mesial region (4) where the decussation angle between
32 alternating rows is the greatest (top panel).

1 **Figure 9. Graphs summarizing distance between rod profiles (spacing) across the four regions of the**
2 **enamel layer within the inner and outer enamel layers and near the CEJ.** Graphs summarizing
3 distance between rod profile (spacing) across the four regions of the enamel layer (1, lateral; 2,
4 mid lateral, 3, central labial; 4, mesial) relative to the inner enamel layer (IE), the outer enamel
5 layer (OE) and near the CEJ. Data are from 24 mandibular incisors of 18 mice; inner enamel N=
6 62,986 mesial tilt, N= 56,337 lateral tilt; outer enamel N= 46,120; CEJ N= 5,183. The tightest
7 packing together of rod profiles occurs in the central labial region (3) of the outer enamel layer
8 (right panel) followed by the central labial and mesial (4) regions of the inner enamel layer for
9 rod profiles having a mesial tilt (left panel). The widest spacing of rod profiles occurs in the
10 mesial region of the inner enamel layer for rod profiles having a lateral tilt (left panel). Rod
11 profile spacing in both the inner and outer enamel layers shows a trend to increase in a lateral
12 direction (region 3 toward region 1) and to increase in a mesial direction but only within outer
13 enamel layer (region 3 toward region 4) Rod profile spacing near the CEJ is similar at the mesial
14 and lateral sides and is intermediate in distance between spacing seen in the inner and outer
15 enamel layers.

16 **Figure 10. Schematic illustration of the multi directional developmental pattern for enamel and the**
17 **step-like arrangement of enamel rods created relative to cross sectional plane of the**
18 **mandibular mouse incisor.** Low magnification BEI image of a cross section of the enamel layer
19 covering the labial side of a mandibular mouse incisor (top left side). The boxed area is shown at
20 higher magnification at the bottom. On the right side are schematic drawings illustrating how
21 enamel rods project into or out of the plane of section to varying degrees depending upon their
22 location across the thickness of the enamel layer. Enamel rod profiles, each representing a
23 single 2D slice out of the much larger 3D enamel rod, found near the DEJ are the most apical
24 starting points for rods projecting mostly in an incisal direction out of the plane of section while
25 rod profiles seen near the outer surface are cut at the incisal end of rods projecting in an apical
26 direction backwards into the tissue block. Rod profiles seen in the middle of the enamel layer
27 would have one-half their 3D length projecting apically and the other half projecting incisally
28 with all other profiles in between projecting predominately incisally (above midpoint) or apically
29 (below midpoint). During development, enamel formation begins near the DEJ at the central
30 side of the tooth (boxed area, location A) and spreads as a wave in a mesial direction (arrow to
31 location B) and lateral direction (arrow to location C) as the enamel layer increases in thickness
32 by appositional growth (arrow to location D) (Smith and Warshawsky, 1976). A cross section of

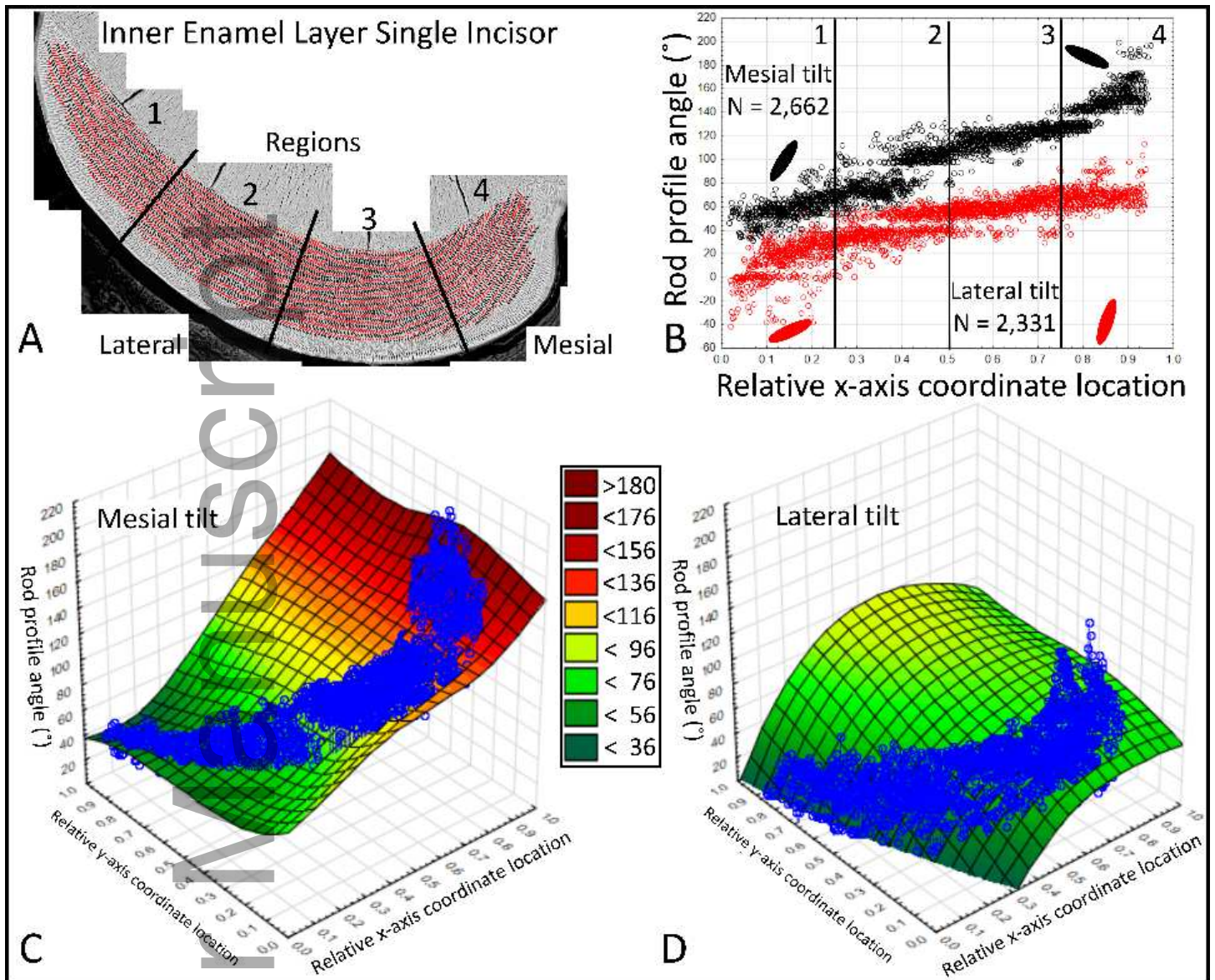
1 the incisor therefore represents a composite image built up over time of the creation of lamellar
2 sheets of rods stacked in a step-like arrangement one behind the other with alternating tilts.
3 This formative process spreads as a wave to the mesial and lateral sides of the labial surfaces so
4 that location A begins its development before location B followed by location C thereby creating
5 a time composite of development cross the whole enamel layer. The thin ring of rod profiles
6 abutting the DEJ and those abutting the outer surface define the entire volume of 3D enamel
7 rod space sampled by the cross section.

Author Manuscript

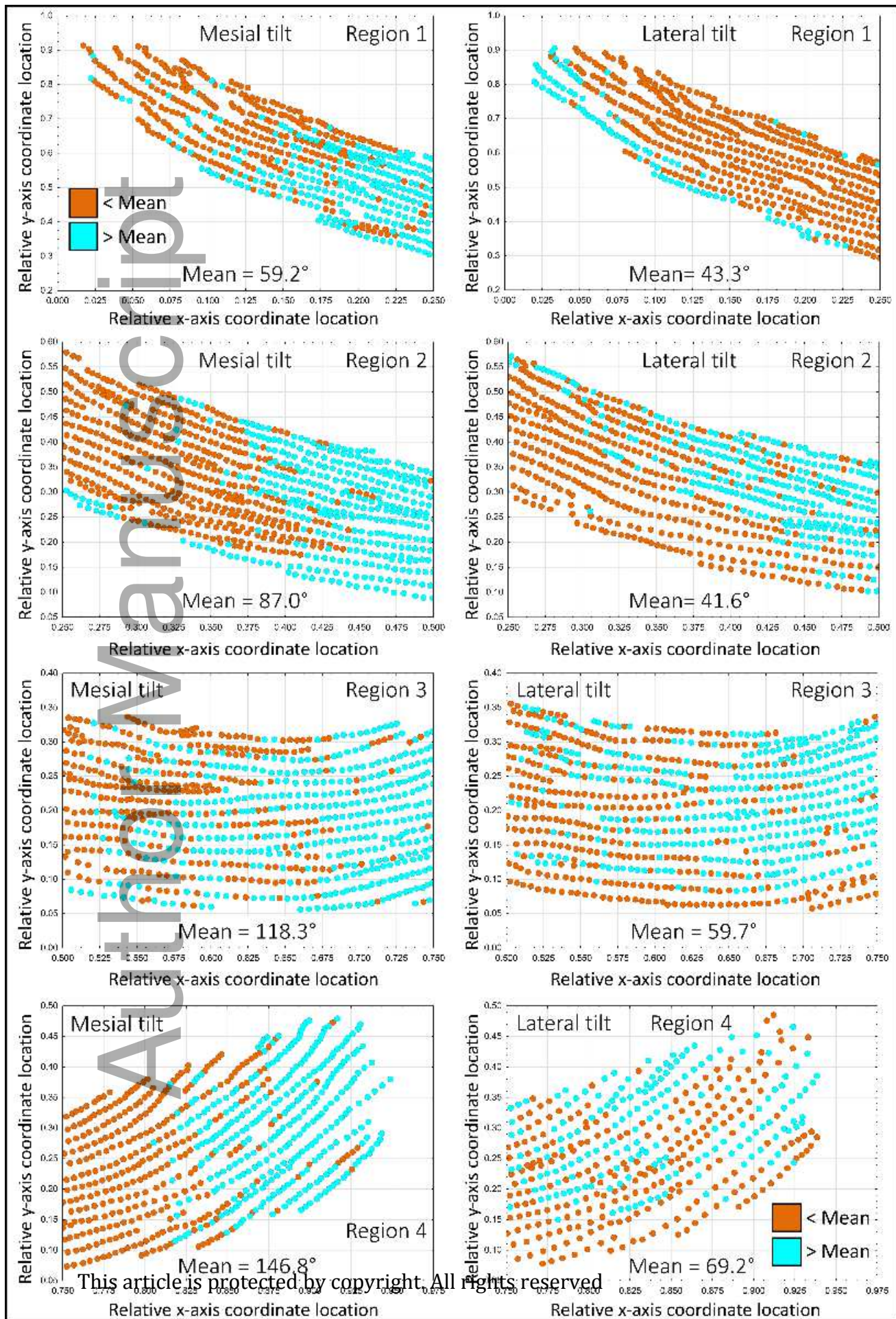


joa_12912_f1.tif

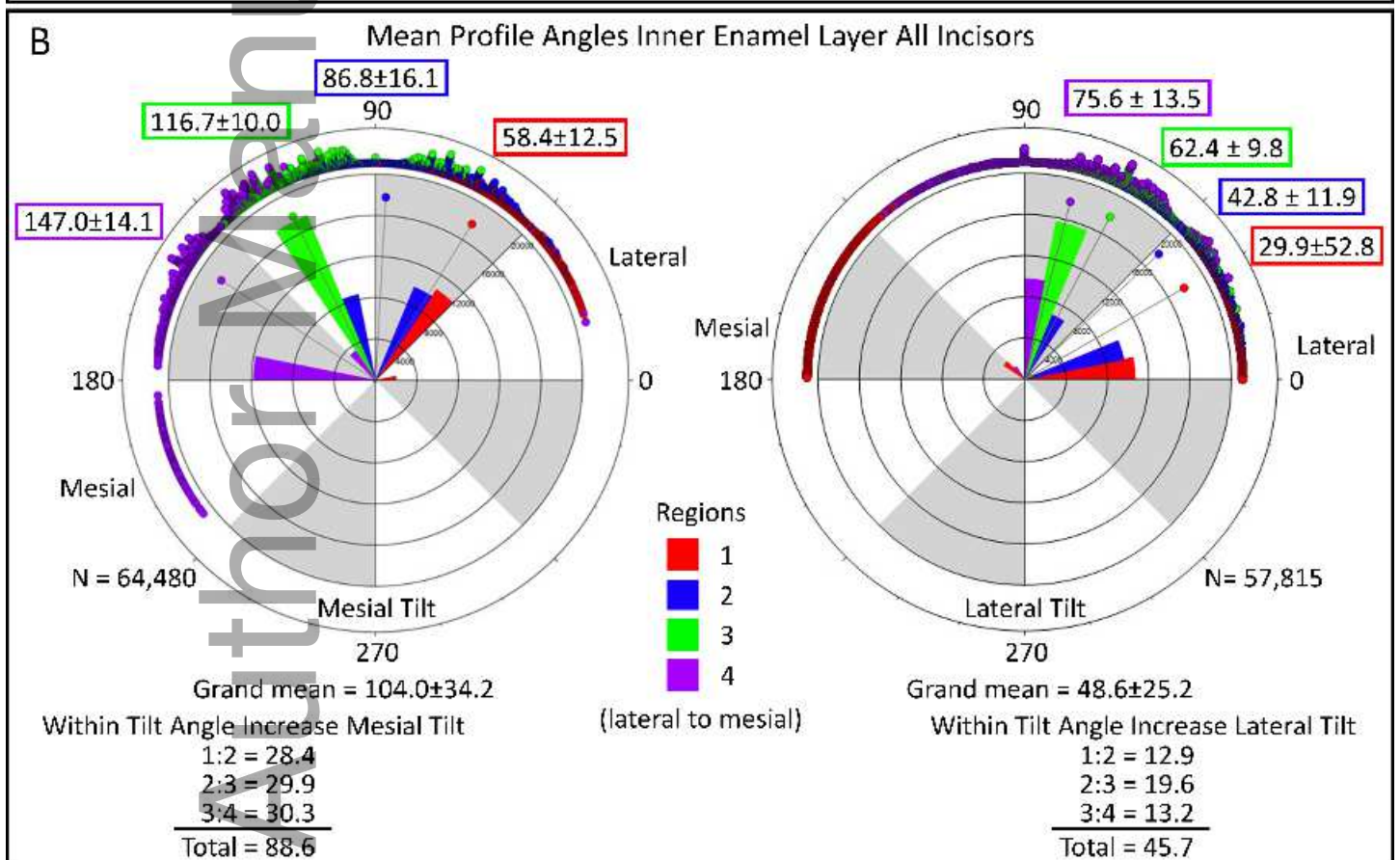
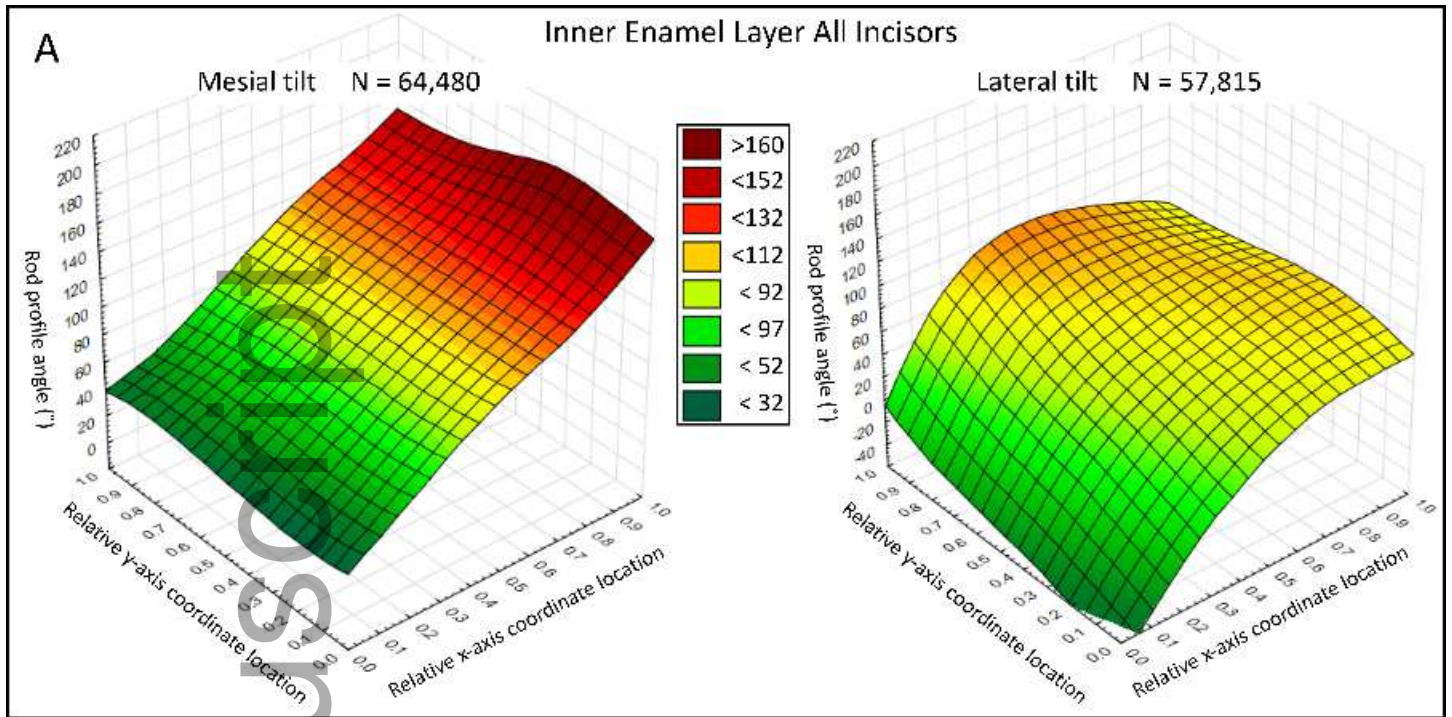
Author Manuscript



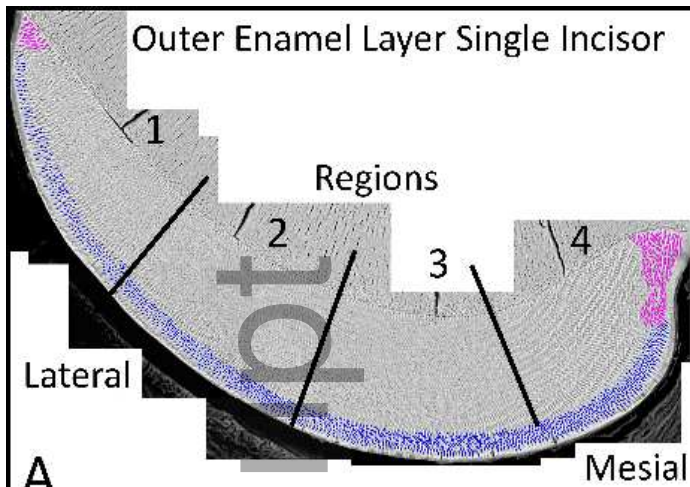
joa_12912_f2.tif



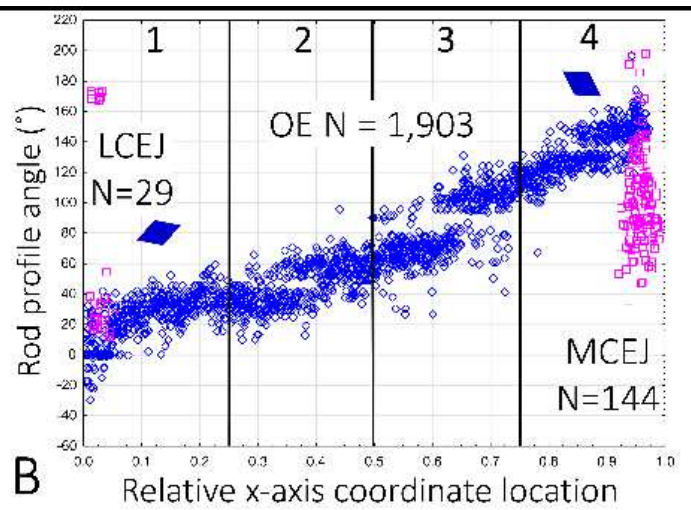
This article is protected by copyright. All rights reserved.



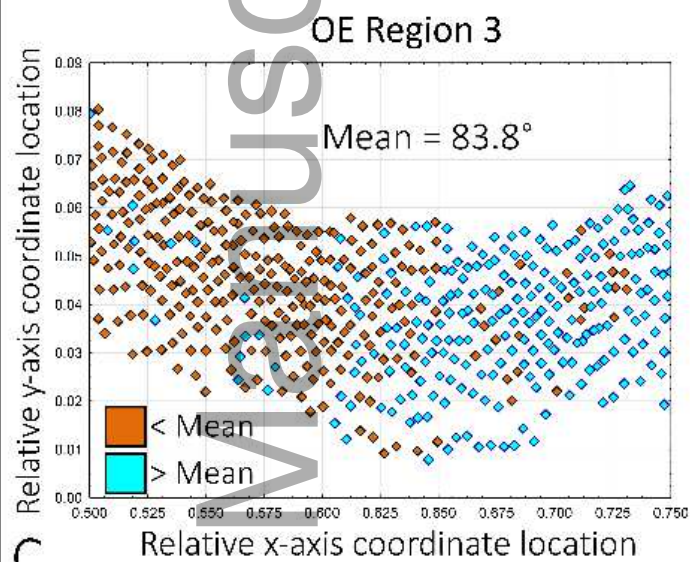
joa_12912_f4.tif



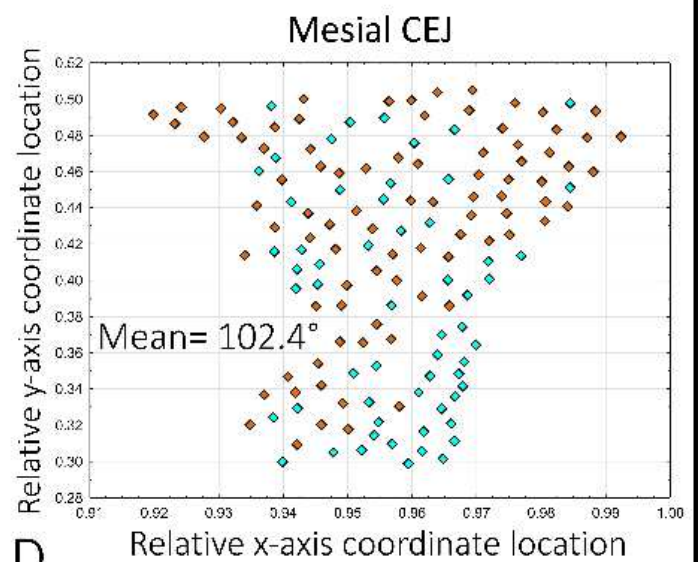
A



B

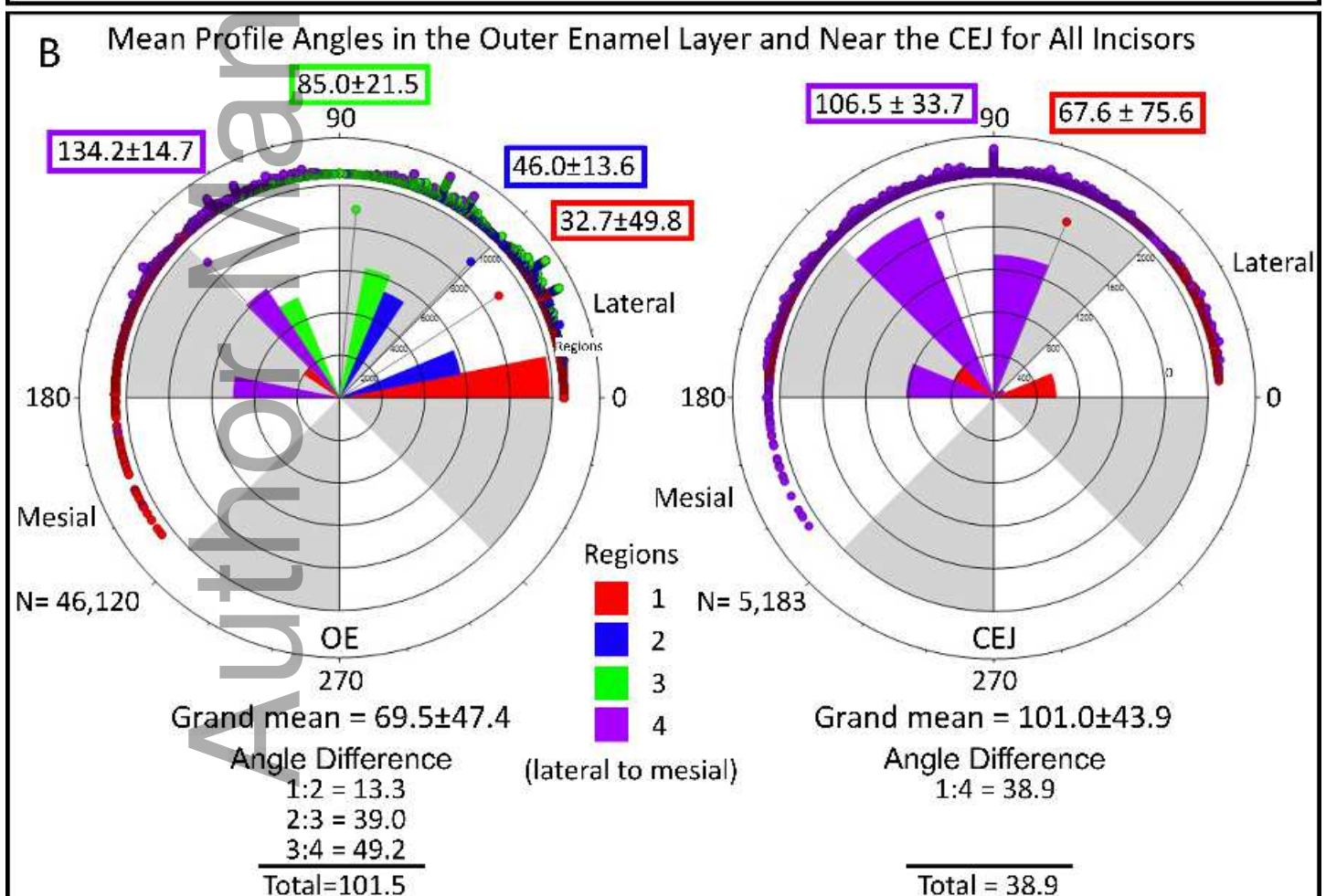
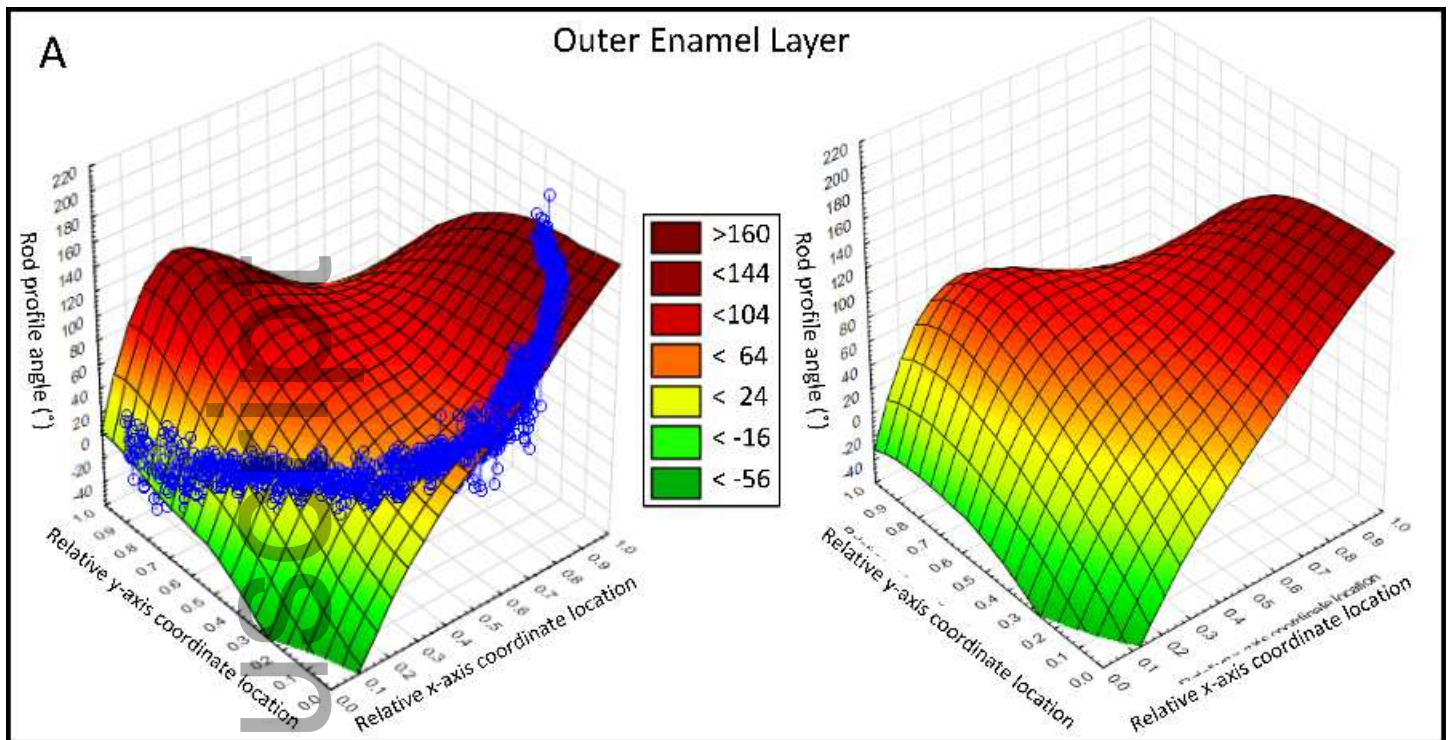


C

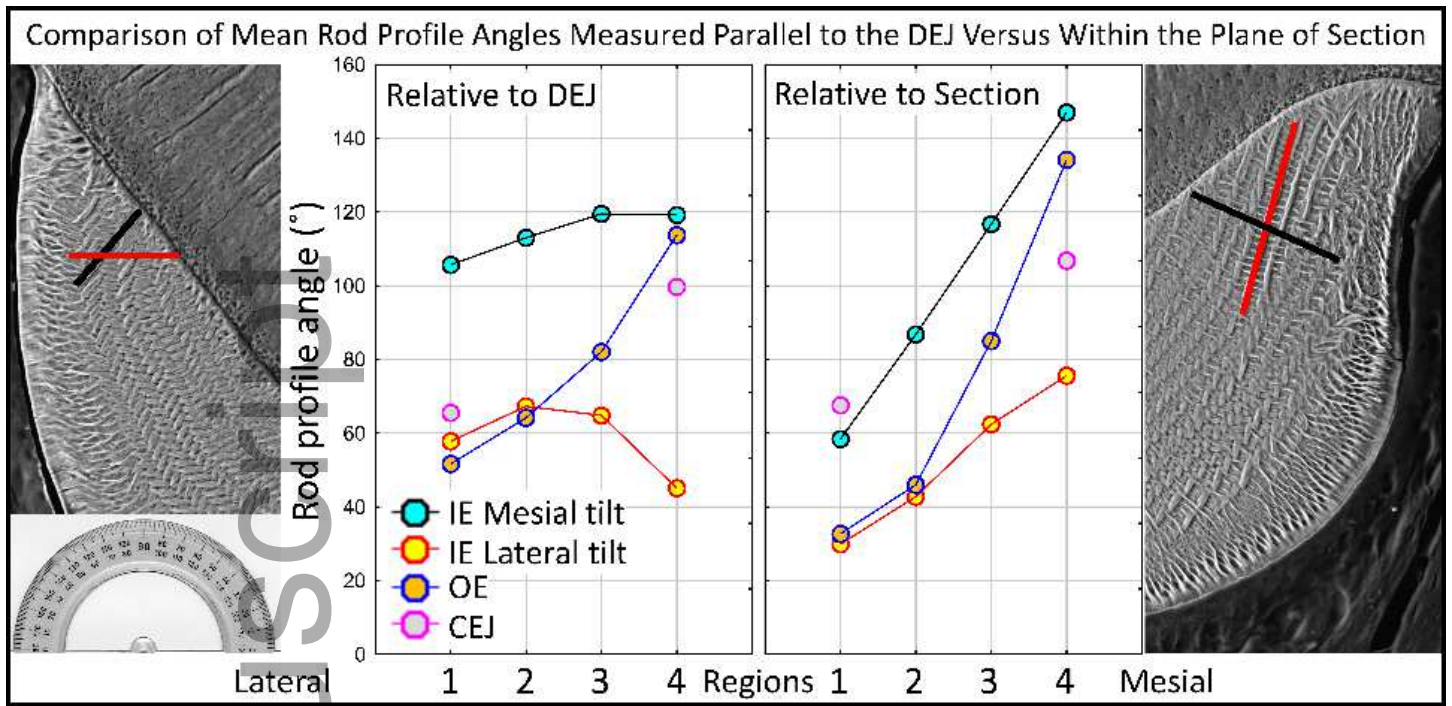


D

joa_12912_f5.tif



joa_12912_f6.tif

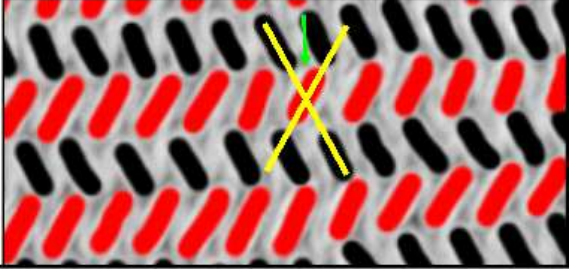
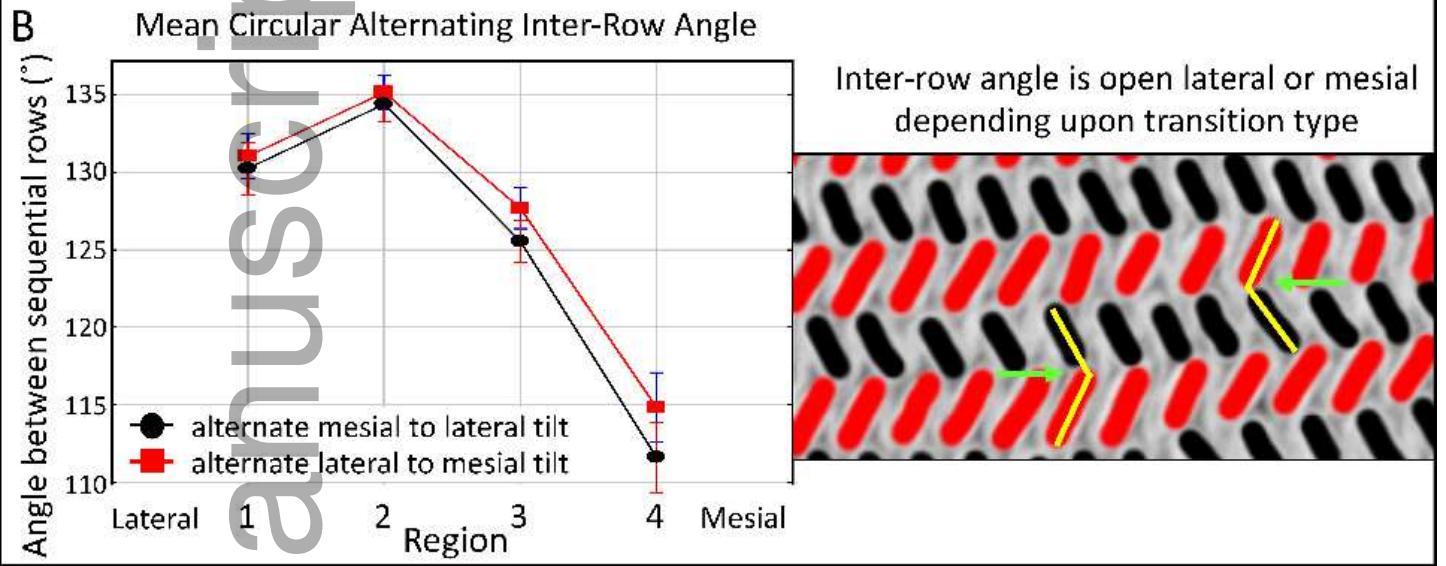


joa_12912_f7.tif

Author Manuscript

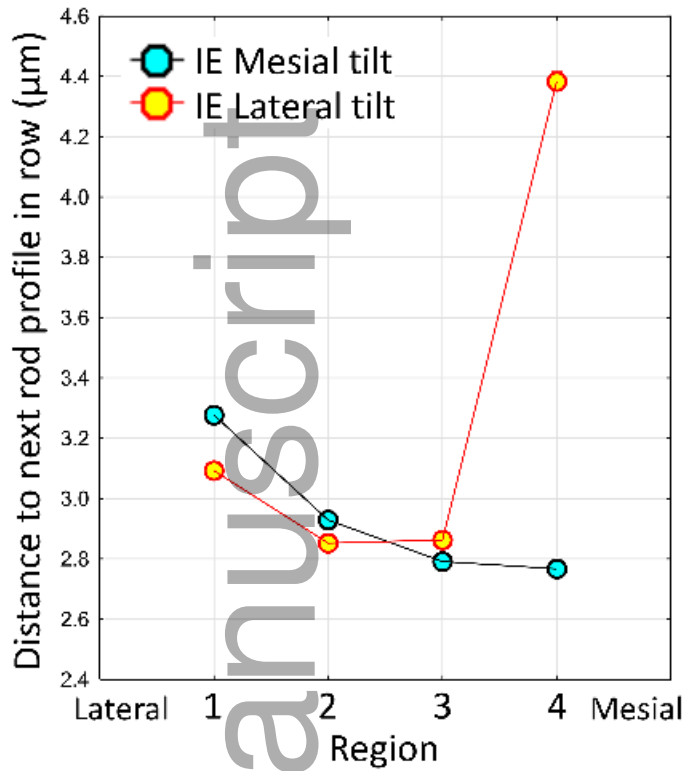
A Mean Circular Decussation Angle Between Alternating Rows Forming the Inner Enamel Layer

Regions	Angle Difference Between Rows			
	(lateral)		(mesial)	
	1	2	3	4
Based on means (Fig. 4)	29°	44°	54°	71°
Relative to DEJ	48°	46°	54°	74°
Relative to Section	42°	43°	43°	70°

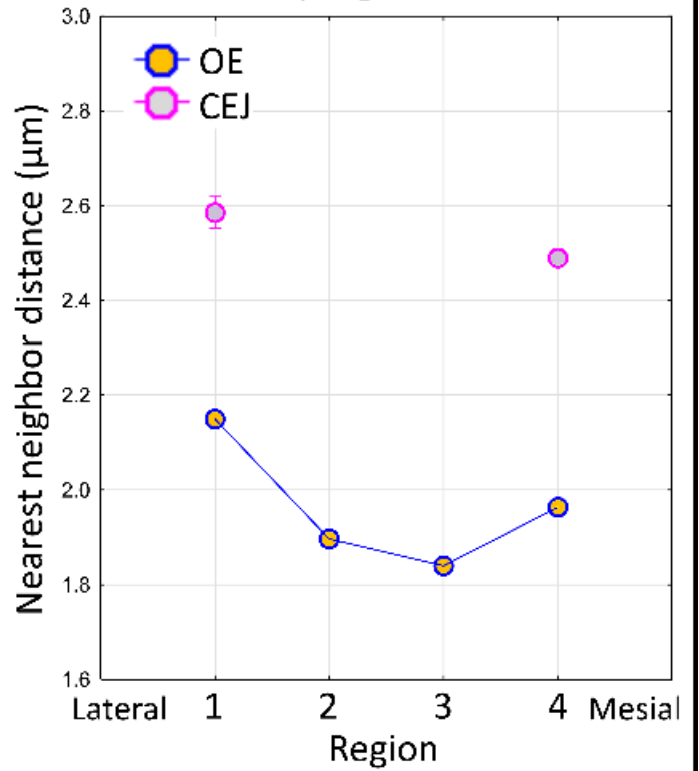



joa_12912_f8.tif

Within Row Spacing of Enamel Rod Profiles in the Inner Enamel by Region for All Incisors

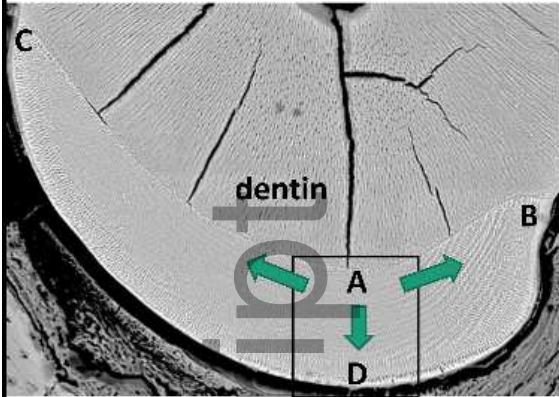


Nearest Neighbor Spacing of Rod Profiles in the Outer Enamel and Sites Near the Mesial and Lateral CEJ by Region for All Incisors

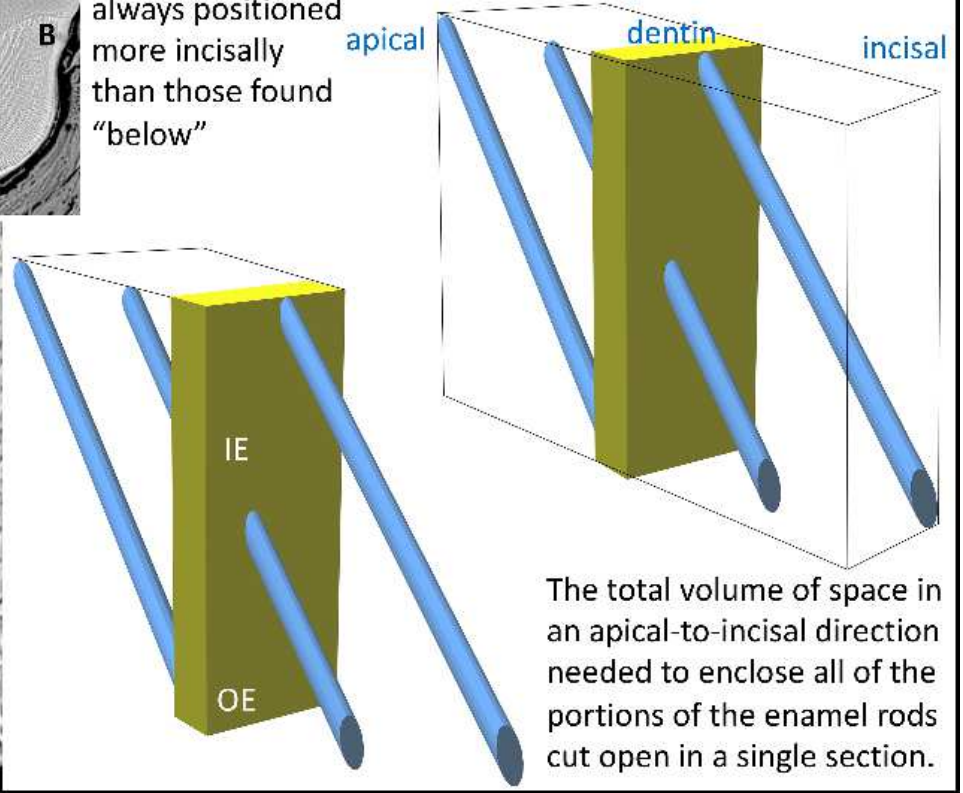
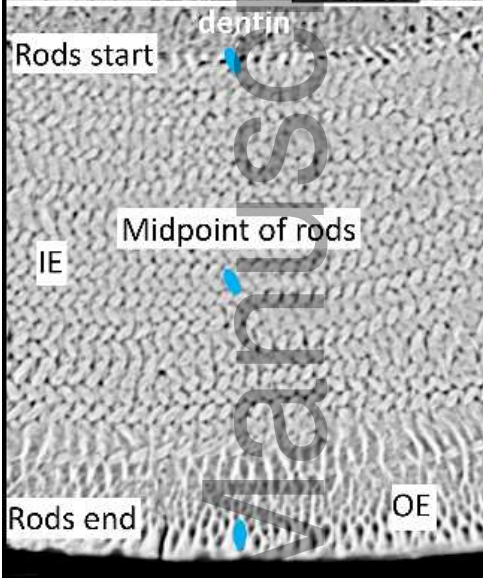


joa_12912_f9.tif

Mosaic Nature of Cross-Sectional Faces Relative to Development



Across the face of a cross section (yellow), enamel rods are sliced open at different levels relative to their overall 3D length creating a staircase effect. From DEJ to the surface, the starting point for rods in a row "above" is always positioned more incisally than those found "below"



joa_12912_f10.tif

Author